Transient Analysis and Control for Scalable Network Systems

Hansson, Jonas

2023

Document Version:
Publisher's PDF, also known as Version of record

Link to publication

Citation for published version (APA):
Hansson, J. (2023). *Transient Analysis and Control for Scalable Network Systems*. [Licentiate Thesis, Department of Automatic Control]. Department of Automatic Control, Lund Institute of Technology, Lund University.

Total number of authors:
1

LUND UNIVERSITY

PO Box 117
221 00 Lund
+46 46-222 00 00

Transient Analysis and Control for Scalable Network Systems

Jonas Hansson

LUND UNIVERSITY

Department of Automatic Control

Licentiate Thesis TFRT-3280
ISSN 0280–5316

Department of Automatic Control
Lund University
Box 118
SE-221 00 LUND
Sweden

Printed in Sweden by Media-Tryck.
Lund 2023

Abstract

The rapidly evolving domain of network systems poses complex challenges, especially when considering scalability and transient behaviors. This thesis aims to address these challenges by offering insights into the transient analysis and control design tailored for large-scale network systems. The thesis consists of three papers, each of which contributes to the overarching goal of this work.

The first paper, *A closed-loop design for scalable high-order consensus*, studies the coordination of n^{th}-order integrators in a networked setting. The paper introduces a novel closed-loop dynamic named *serial consensus*, which is designed to achieve consensus in a scalable manner and is shown to be implementable through localized relative feedback. In the paper, it is shown that the serial consensus system will be stable under a mild condition – that the underlying network contains a spanning tree – thereby mitigating a previously known scale fragility. Robustness against both model and feedback uncertainties is also discussed.

The second paper, *Closed-loop design for scalable performance of vehicular formations*, expands on the theory on the serial consensus system for the special case when $n = 2$, which is of special interest in the context of vehicular formations. Here, it is shown that the serial consensus system can also be used to give guarantees on the worst-case transient behavior of the closed-loop system. The potential of achieving string stability through the use of serial consensus is explored.

The third paper, *Input-output pseudospectral bounds for transient analysis of networked and high-order systems*, presents a novel approach to transient analysis of networked systems. Bounds on the matrix exponential, coming from the theory on pseudospectra, are adapted to an input-output setting. The results are shown to be useful for high-order matrix differential equations, offering a new perspective on the transient behavior of high-order networked systems.

Acknowledgements

First and foremost, I owe a deep gratitude to Emma. The countless late-night research sessions, the knack for identifying intriguing problems, and the genuine partnership we've formed in our academic journey have been pivotal. Your support and guidance have been invaluable to my progress. I'd also like to thank Anders, for always being open to discussing new ideas and providing insight.

Now, to the Department of Automic Control in Lund. Where to start? Fika at 10? Coffee at 15? Why not both? Great technical staff, or superb administrative staff? Why not both? An intense game of floorball, or perhaps a nerve-wracking night with boardgames – we even have intellectually stimulating study circles! I am blessed to work in such a great environment.

Some random words: Atlanta, Cancún, Paris, Austria, and the Netherlands. I eagerly look forward to the coming adventures – guess it's Singapore next!

Lastly, a huge thanks to Linnéa and my family. Your support and encouragement have been invaluable to me. All love.

Contents

1

Introduction

All around the world we can see large and complex networked systems emerge. Some examples are power grids, transportation networks, and flocking of animals. Much of our understanding of such systems comes from the study of their steady-state behavior and the stability of this behavior. While this is fundamental – both good steady-state behavior and stability are necessary for a system to be well-behaved – in many cases the transient behavior may be of equal importance. For instance, in the case of a vehicle platoon as illustrated in Fig. 1.1, the transient behavior may determine weather the vehicles of the platoon will collide or not. To see this, consider the simple vehicle model

$$\ddot{x}_i(t) = u_i(x,t).$$

That is the vehicles are assumed to be identical point-masses which will accelerate proportional to their control input $u_i(x,t)$. Now, a simple control strategy would be to let the control input be proportional to the relative distance and relative velocity to the vehicle in front of it, i.e.

$$u_i(x,t) = r_0(x_{i-1}(t) - x_i(t) - d_i) + r_1(\dot{x}_{i-1}(t) - \dot{x}_i(t)),$$

where d_i is a desired distance that agent i should keep to the vehicle in front of it. These position errors can be mesured through an onboard radar, something modern commercial vehicles are already equipped with. By analysing the poles of this system one can conclude that the system will be stable if $r_0, r_1 > 0$ and this is independent of the number of vehicles. Thus, all vehicles will eventually settle at the desired intervehicle distances. However, as illustrated in Fig. 1.2, when the

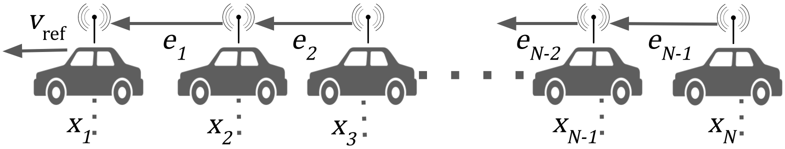

Figure 1.1 Illustration of a vehicle platoon.

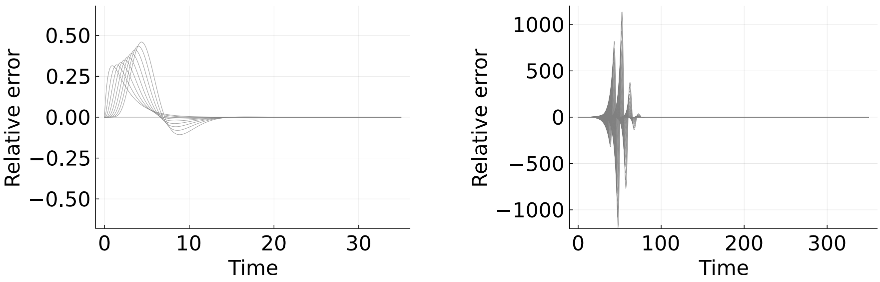

(a) Simple control of formation with 10 vehicles.

(b) Simple control of formation with 100 vehicles.

Figure 1.2 The lead vehicle in the formation changes its velocity. The deviation from the desired intervehicle distance throughout the transient phase are shown. When the number of vehicles increases the largest deviation increases. Clearly, the vehicles in the 100 vehicle platoon will collide during the transient.

number of vehicles increases, then so will also the local deviations throughout the transient phase. This behavior is known in the literature as *string-instability*, see e.g. [Swaroop and Hedrick, 1996; Stüdli et al., 2017; Abolfazli et al., 2023; Feng et al., 2019; Seiler et al., 2004], and is a spectacular example of a lack of *scalability* of the control deisgn to large formations.

The problem of string-instability is, in fact, not only a theoretical problem. In a recent test of commercial cruise control systems [Gunter et al., 2021] they found that all seven tested systems had problems with controlling the transient and could not be considered string-stable. Like in the example above, this means that small errors in the speed and relative distances between the vehicles would get amplified and propagated throughout the platoon. Clearly, this indicates that there is a need for better understanding of the transient behavior of networked systems. While this problem is particularly easy to grasp in the scenario of a string of vehicles, the issue of error propagation or cascading failures is relevant to many engineered network systems with other topologies, and a generalization of the notion of string stability to meshed networks has also been proposed in e.g. [Besselink and Knorn, 2018].

1.1 Aims of the thesis

This thesis aims to study the behavior of large-scale networked linear systems when controlled through relative feedback. In particular, emphasis is put on three aspects: 1) the transient behavior of such systems, 2) the design of scalable controllers that ensures good performance and robust stability also as networks grow large, and 3) the development of a theoretical framework for the analysis of transient behavior, for control systems in general and network systems in particular.

2

Background

2.1 Modelling of networked dynamical systems

In many applications, the dynamics of a networked system can be described by considering a set of N interconnected subsystems. When the subsystems are similar, such as in the case of a formation of vehicles, swarms of drones, or a network of power generators, it is often convenient to describe the dynamics of the entire network using a single dynamical model which captures the essential behavior of the individual subsystems. For instance, in the case of a formation of vehicles, the dynamics of each vehicle can be described by a double integrator model which follows from Newton's second law. The collective dynamics of the formation can then be described by the simple model

$$M\ddot{x} = u(x,t),$$

where $x(t) \in \mathbb{R}^N$ is the state representing the positions of the vehicles, $M \in \mathbb{R}^{N\times N}$ is a positive definite diagonal mass matrix, and $u(x,t) \in \mathbb{R}^N$ is the control input. Of course this model is a simplification of the real system, but it captures the essential behavior of the system. In any case, understanding the behavior of this model is a good starting point for understanding the behavior of the real system. A slightly more general model is given by

$$A_n x^{(n)}(t) + A_{n-1}x^{(n-1)}(t) + \cdots + A_1\dot{x}(t) + A_0 x(t) = u(x,t), \tag{2.1}$$

where $A_k \in \mathbb{R}^{N\times N}$ for $k = 0, 1, \ldots, n$ are constant matrices and $x^{(k)}(t)$ denotes the k^{th} derivative of $x(t)$. This model is general enough to capture the dyanamics of many networked systems. Even in the case of nonlinear systems, it is often possible to approximate the dynamics by a linear model around some desired operating point.

2.2 Controlling networked dynamical systems

A core objective of a control design is to ensure that a system behaves well around operating points and follow desired trajectories, even when disturbances and uncertainties are present (which they always are). When controlling large networked

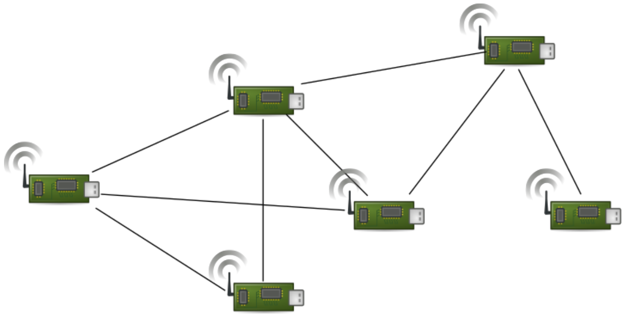

Figure 2.1 A system consisting of $N = 6$ interconnected subsystems, where the connecting lines represent communication links.

dynamical systems an additional constraint arrises, namely that the control input is often required to be distributed. This means that each subsystem can only use information from its neighbors to compute its control input. This is due to the fact that a centralized controller would require very large communication and computation resources, which may not be possible to implement in practice.

The constraint of distributed control can be formulated as follows. Let $\mathcal{G} = (\mathcal{V}, \mathcal{E})$ be a graph with vertex set $\mathcal{V} = \{1, 2, \ldots, N\}$ and edge set $\mathcal{E} \subseteq \mathcal{V} \times \mathcal{V}$. The graph $\mathcal{G}$ represents the communication topology of the networked system, an example of which is presented in Fig. 2.1. The edge $(i, j) \in \mathcal{E}$ indicates that agent i can communicate with agent j. The set of neighbors of agent i is denoted $\mathcal{N}_i$. With this notation, a general linear state feedback controller for system (2.1) can be written as

$$u_i(x,t) = u_{i,\mathrm{ref}}(t) - \sum_{k=0}^{n} \sum_{j \in \mathcal{N}_i} b_{ij}^{(k)} x_j^{(k)}(t), \tag{2.2}$$

where $u_{i,\mathrm{ref}}(t)$ is the desired control input for agent i and $b_{ij}^{(k)} \in \mathbb{R}$ for $k = 0, 1, \ldots, n$ and $(i, j) \in \mathcal{E}$ are constant gains. Further constraints can then be placed on the b_{ij} to capture the permissible feedback. Throughout this thesis, we will often consider relative feedback, which implies that $\sum b_{ij} = 0$. Relative feedback, arising through diffusive couplings or measurement equipment, like radars, that measure differences in states, is prevalent in applications and known to be limiting to control of large-scale systems, see e.g. [Bamieh et al., 2012; Tegling, 2018; Jensen and Bamieh, 2022].

Systems which can be formulated as (2.1) and are controlled with a controller of the form (2.2) make up a large class of networked dynamical systems. This type of systems and the solutions thereof will be the focus of this thesis.

2.3 Solutions of linear systems

It turns out that the networked dynamical system that was outlined in the previous section is a special case of a linear time-invariant system. The closed-loop system can be written as

$$\dot{\xi}(t) = \underbrace{\begin{bmatrix} 0 & I_n & 0 & \dots \\ \vdots & \ddots & \ddots & 0 \\ 0 & \dots & 0 & I_n \\ -A_0 - B_0 & -A_1 - B_1 & \dots & -A_{n-1} - B_{n-1} \end{bmatrix}}_{\mathcal{A}} \xi(t) + \underbrace{\begin{bmatrix} 0 \\ \vdots \\ 0 \\ B \end{bmatrix}}_{\mathcal{B}} u_{\text{ref}}(t) \tag{2.3}$$
$$y(t) = \mathcal{C}\xi(t).$$

where $\xi(t) \in \mathbb{R}^{Nn}$ is the state vector, $u_{\text{ref}}(t) \in \mathbb{R}^N$ is the reference input, $y(t) \in \mathbb{R}^N$ is the output, and $\mathcal{A}$, $\mathcal{B}$, and $\mathcal{C}$ are constant matrices. The solution of a linear time-invariant system of the form (2.3) is well known and can simply be written as

$$y(t) = \mathcal{C}e^{\mathcal{A}t}\xi(0) + \int_0^t \mathcal{C}e^{\mathcal{A}(t-\tau)}\mathcal{B}u_{\text{ref}}(\tau)\mathrm{d}\tau.$$

2.4 The consensus problem

A particular case of a networked dynamical system is the consensus problem The idea here is that each agent is allowed to observe the relative distances between itself and its neighbors and then make a control effort which depends on these relative distances. This can then lead to the agents reaching a common state, i.e., a consensus. One of the simplest controllers which can be used to achieve consensus is the linear consensus protocol, which has been studied extensively in the literature, see e.g. [Young et al., 2010; Patterson and Bamieh, 2014; Siami and Motee, 2016]. The linear consensus protocol is given by

$$\dot{x}(t) = -Lx(t) + u_{\text{ref}}(t), \text{ where } x(0) = x_0 \tag{2.4}$$

where $x_0 \in \mathbb{R}^{N\times N}$ is the initial condition and L is a, potentially weighted, graph Laplacian matrix. L can formally be defined as

$$L = D - W,$$

where D is a diagonal matrix with $D_{ii} = \sum_{j=1}^N W_{ij}$ and W is a weighted adjacency matrix of the graph $\mathcal{G}(\mathcal{V},\mathcal{E})$, i.e. $W_{i,j} > 0 \iff (i,j) \in \mathcal{E}$. It turns out that the linear consensus protocol possess some interesting properties. For example, under the relatively mild constraint that the graph $\mathcal{G}$ contains a directed spanning tree, then this controller will drive the agents to a consensus, i.e., $\lim_{t\to\infty} x_i(t) - x_j(t) = 0$ for all $i, j \in \mathcal{V}$ [Ren et al., 2007a]. Or in other words, the solution of (2.4) will converge to a state $x(t) \in \mathrm{span}(\mathbf{1})$, where $\mathbf{1}$ is the consensus vector of all ones. Furthermore, the solution of (2.4) will be contractive in the $\|\cdot\|_\infty$-norm, i.e., $\|x(t)\|_\infty \leq \|x_0\|_\infty$ for all $t \geq 0$ [Willems, 1976]. Lastly, since the stability of the linear consensus protocol only depends on the existence of a directed spanning tree, it follows that additions of new measurements to an already existing network will not affect the stability of the system. These properties are very desirable in many applications, and the linear consensus controller has therefore received ample attention in the literature, see e.g. [Siami and Motee, 2016; Young et al., 2010].

In the case of formation control, the agents should of course not reach the same position, but rather a fixed formation with desired inter-agent distances. This can however be achieved by simply adding a constant offset vector to the controller. To see this, consider $\hat{x} = x - p_x$, where p_x is a desired position. Then, the dynamics of $\hat{x}$ is given by

$$\dot{\hat{x}} = -L(x - p_x) - Lp_x + u_{\mathrm{ref}} = -L\hat{x} + (u_{\mathrm{ref}} - Lp_x)$$

which is of the same form as (2.4) with $u_{\mathrm{ref}} - Lp_x$ as the new reference input. Hence, the agents will reach a consensus with the desired offset with this simple controller.

2.5 High-order consensus

The linear consensus protocol can be used to coordinate a group of agents to a common state. However, the agents will not be able to track a reference trajectory with this simple controller. Though, there is a generalisation of the linear consensus protocol which allows the agents to track a reference trajectory. This generalisation is called the *high-order consensus* protocol, as considered in [Ren et al., 2007b]. Here, the control of N identical n^{th}-order integrator systems is considered. The dynamics can be compactly written as

$$x^{(n)}(t) = u_{\mathrm{ref}}(t) - \sum_{k=0}^{n-1} -L_k x^{(k)}(t) \text{ where } x^{(k)}(0) = x_0^{(k)}, \tag{2.5}$$

where $x_0^{(k)} \in \mathbb{R}^N$ is the initial condition for the k^{th} derivative of the state and L_k is a, potentially weighted, graph Laplacian matrix.[1] This problem has also been studied in e.g. [Jiang et al., 2009; Rezaee and Abdollahi, 2015; Radmanesh et al., 2017]. In [Tegling et al., 2023] it was shown that the high-order consensus protocol may lead to an unstable closed-loop system unless the local gains for each agent is tuned

[1] For simplicity, a scalar state x is considered, making longitudinal control the problem of interest. With a higher-dimensional agent state, the control (2.5) can be applied in all coordinate directions, provided the agents are point masses and the control can be decoupled. For non-holonomic agents, it is slightly more involved, and outside the scope of this thesis.

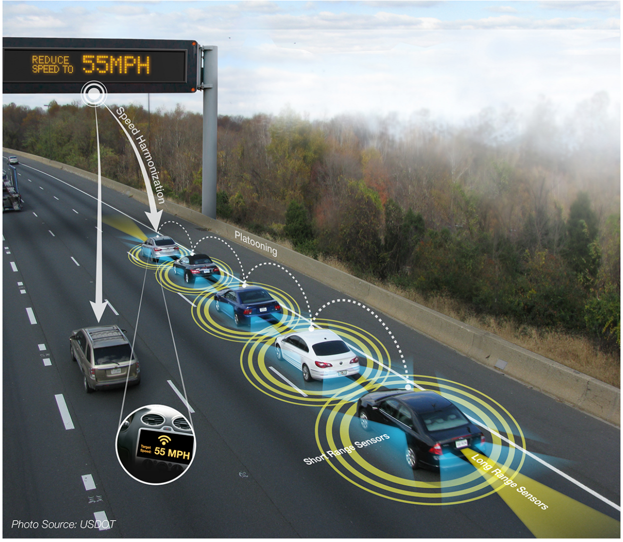

Figure source: U.S. Department of Transportation, 2015

Figure 2.2 Illustration of a vehicle formation.

with respect to the eigenvalues of the graph Laplacian. Thus, the underlying graph structure in the feedback plays a crucial role, for the stability of the closed-loop system.

Another property of the high-order consensus protocol is the existence of an n^{th}-order integrator, even in the closed-loop system. This makes the system unstable. Thus if one were to analyze or bound the norm of the associated solution operator $e^{\mathcal{A}t}$, one would inevitably find out that $\sup_{t\geq 0} \|e^{\mathcal{A}t}\| = \infty$. In this scenario, the n^{th}-order integrator is designed to be associated with the consensus vector and is there to allow the formation to track more complex trajectories. It is therefore interesting to also study the behavior around the consensus vector, and the transient in particular. This motivates the need for results which can describe the behavior of $\mathcal{C}e^{\mathcal{A}t}\mathcal{B}$ for $t \geq 0$, where $\mathcal{A}$ is the closed-loop system matrix, $\mathcal{B}$ is the input matrix, and $\mathcal{C}$ is the output matrix, that makes the output orthogonal to the consensus vector.

2.6 Vehicle formation control

A particularly interesting case of the high-order consensus protocol is when the agents are modeled as dobule integrators. The double-integrator system can be seen as a simple vehicle model which is often used in the literature on vehicle formation control and in particular vehicle platooning, see e.g. [Barooah et al., 2009; Andreasson et al., 2014; Hao and Barooah, 2013; Herman et al., 2017]. An illustrating figure of a vehicle formation is shown in Figure 2.2. For the vehicle platoon problem, the goal is to coordinate a group of vehicles to maintain fixed intervehicle distances while moving at the same velocity. For large vehicle formations, it may not be feasible for all vehicles to keep track of a global reference or properties such as the number of agents in the formation. Local and relative measurements can however be used and communicated locally. Thus, an important aspect of the vehicle platoon problem is to design a distributed controller which adheres to these constraints. As for the general high-order consensus protocol, there will be an unstable subspace in the closed-loop system. This subspace corresponds to the consensus equilibrium where the vehicles are moving at the same velocity and with fixed intervehicle distances. So in this case it is also interesting to study the behavior of the solution around this equilbrium. In the case of vehicle platoons, it is especially interesting to study the transient of the intervehicle distances $e_p(t) = Lx(t)$, where L is a graph Laplacian matrix which encodes the relative errors. These relative errors must remain bounded throughout the transient in order to guarantee that the vehicles do not collide. Another interesting error to study is the velocity error $e_v(t) = \dot{x}(t) - v_{\text{ref}}\mathbf{1}$. This error must also remain bounded to guarantee that the vehicles do not exceed the speed limits. This problem is addressed in Paper II.

3

Contributions

3.1 Paper I

This paper tackles the problem of coordinating a group of N identical n^{th}-order integrator systems and thus the design of the controller $u(x,t) \in \mathbb{R}^N$ in

$$\frac{\mathrm{d}^n x(t)}{\mathrm{d}t^n} = u(x,t).$$

The controller is restricted to only use local, linear and relative state measurements. A new control law is proposed which is called the *serial consensus* controller. The controller is chosen to achieve the desired closed-loop dynamics

$$\left(\prod_{k=1}^{n} sI + L_k\right) X(s) = U_{\text{ref}}(s),$$

here expressed in the Laplace domain. This system can be proven to be stable around the consensus equilibrium under the mild constraint that the graphs underlying the graph Laplacians L_k each contain a spanning tree. This addresses a previously observed scalability issue with the high-order consensus protocol, where stability can not be guaranteed for large networks. The proposed serial consensus controller is shown to satisfy the requirements on locality and use of relative measurements. In the case where each Laplacian matrix L_k only encodes feedback between neighboring agents, then the relative measurements needed to implement the serial consensus controller is shown to be confined to an n-hop neighborhood of each agent.

The control design is further motivated through its robustness properties. Through the use of the well-known small-gain theorem, it is shown that the closed loop system is robust to both model and feedback uncertainties. This makes the stability properties of the closed-loop system also applicable to a real-world implementation where there inevitably is uncertainty, both in agent-model and in the feedback. The findings are also illustrated through examples.

This paper will appear in the proceedings of the 2023 IEEE Conference on Decision and Control.

3.2 Paper II

Paper II expands on the work of Paper I by analyzing the performance of the second order serial consensus system, which is relevant in the context of vehicle formations. Given any graph Laplacian L which defines a set of relative errors $e_p(t) = Lx(t)$ and absolute velocity deviation $e_v(t) = \dot{x}(t) - \mathbf{1}v_{\text{ref}}$ then the serial conensus system

$$\ddot{x}(t) = -(p_1 + p_2)L\dot{x}(t) - p_1 p_2 L x(t)$$

can be shown to guarantee that

$$\sup_{t\geq 0}\left\|\begin{bmatrix} e_p(t) \\ e_v(t)\end{bmatrix}\right\| \leq \alpha(p_1, p_2)\left\|\begin{bmatrix} e_p(0) \\ e_v(0)\end{bmatrix}\right\|$$

where $\alpha(p_1, p_2) < \infty$ as long as $p_1, p_2 > 0$ and $p_1 \neq p_2$. The result is, remarkably, independent of the number of agents and the graph structure. Different choices of graph structures are discussed and illustrated through examples and is contrasted with the conventional consensus controller.

This paper is in preparation for a journal submission.

3.3 Paper III

In this work bounds on the transient behavior of

$$\sup_{t\geq 0} \|\mathcal{C}e^{t\mathcal{A}}\mathcal{B}\|,$$

are derived based on the size of the transfer matrix $\|C(sI - \mathcal{A})\mathcal{B}\|$, measured in the same submultiplicative norm. The proof ideas originate from the pseudospectra literature and are adapted to an input-output setting. The bounds are shown to be particular interesting for analyzing high-order systems, in particular those that can be described by high-order matrix differential equations. One particular example, which is also illustrated in the paper, is the vehicle platooning problem. In this case, the closed-loop system can be modeled as the following matrix differential equation

$$s^2 X(s) + sL_1 X(s) + L_0 X(s) = BU(s),\ Y(s) = CX(s).$$

The new bounds adresses two particular issues of analyzing the transients of this type of systems through the pseudospectra of $\mathcal{A}$. 1) Due to the existence of a double integrator in the system, there will be states drifting to infinity, which implies $\sup_{t\geq} \|e^{tA}\| = \infty$. 2) Since the upper bound of the Kreiss theorem scales linearly with the number of states associated with $\mathcal{A}$, which makes it impossible to determine important properties, such as string stability for large-scale systems. The new bounds are shown to be useful for both these issues.

This paper is published in the proceedings of the 2022 IEEE Conference on Decision and Control.

3.4 Contributions not included in the thesis

The following papers by the author are not included in the thesis, but are here briefly summarized.

- The paper *Limitations of time-delayed case isolation in heterogeneous SIR models* [Hansson et al., 2022] studies the effects of including time delays and heterogeneity, in the contact network, and how these impact the spread of a disease as predicted by the well-known SIR-model.
- In the paper *Next Generation Relay Autotuners – Analysis and Implementation* [Hansson et al., 2021], a short relay experiment is proposed for the identification of a low-order model that can be used for tuning of PI and PID controllers. The experiment was implemented and evaluated in an industrial controller.

4

Discussion and Directions for Future Work

In this thesis, the control of linear time-invariant networked systems has been studied. These make up a large class of systems that are of both theoretical and practical interest, especially in relation to the existing theory on vehicle formations, power grids, and multi-robot networks.

The main contributions have been the introduction of the serial consensus system, a novel control scheme for high-order integrator systems with scalable robustness and stability guarantees, and the generalization of transient bounds, found in the pseudospectra literature, to an input-output setting.

This chapter presents a discussion of the significance, and limitations, of the results and their implications for future research.

4.1 Discussion

Double-integrator networks

In Paper II the problem of coordinating a network of double integrators was considered. The double integrator serves as a simple vehicle model. Despite its simplicity, the double integrator is a common model, especially when considering the scalability of vehicle formations. For future work, it would be interesting to investigate how the serial consensus system scales, for instance when subject to time-delays like in [Darbha et al., 2019]. Another interesting direction is that of time-varying networks, which has been studied in e.g. [Hendrickx and Martin, 2017]. Unlike the conventional consensus, it is possible to use directed graphs in the serial consensus controller and still guarantee string stability. However, this comes at the cost of the agents needing to communicate with their neighbors. In the special case where an ahead-looking string graph is considered, then it will hold that any agent's movement is unaffected by their followers' actions. This property might facilitate the analysis of time-varying networks.

High-order integrator networks

Unlike the network of double-integrators, networks, of high-order integrators where $n \geq 3$ is not as commonly encountered, although they have been used to model coordination of flying objects [Ren et al., 2007a]. They arise, however, when considering PID control of a network of vehicles or other second-order agents. Combining the ideas of Paper I and Paper II, it may be possible to describe the transients of such a system. Besides this, the high-order integrator networks are of theoretical interest since they are a natural generalization of the consensus problem.

Transient analysis

A great emphasis has been put on the transient analysis of dynamical systems. The transient of any dynamical system is interesting, especially of linear models. Since linear models often constitute an idealized version of reality, the transient analysis can be seen as a tool for testing whether one can expect the linearization point to be a good approximation of the real system. Another reason to consider the transient is their importance for keeping systems within a safe operation condition. The bounds presented in Paper III generalize the well-known Kreiss bounds to an input-output setting. However, like the Kreiss bounds, the new bounds are limited to describe impulse and initial-value responses. These can capture the behavior due to some disturbances, but not all. An avenue for future research is to use the bounds of Paper III to describe the performance of network systems in terms of $\mathcal{L}_1$-norms, which due to their intractability have not received sufficient attention in the control community.

Robustness

The robustness results, which are proven in Paper I, deserve some discussion. Firstly, the strength of them lies in the fact that the bounds are, in some sense, independent of the formation size. This is due to them being quantified in terms of the $\mathcal{H}_\infty$-norm of the perturbation blocks. In the case where the uncertainty can be described by a diagonal, or sparse matrix, then the permissible uncertainty is independent of the formation. This is for instance the case for time-delays, but also for vehicle model uncertainty. Although the serial consensus has a particular algebraic structure, the robustness results show that the beneficial properties of the serial consensus does not require a perfect implementation.

For potential future work, it is interesting to consider how the robustness can be used to design controllers with both performance and robustness guarantess. Earlier works have considered how small perturbations can drastically change the algebraic connectivity of the graph Laplacian [Barooah et al., 2009]. If this can be achieved within the robustness framework of Paper I, i.e. through perturbing a serial consensus system, which is based on symmetric matrices, additional slack can then be left to handle other uncertainties.

Scalability

A core theme throughout this thesis is that of scalability. In the setting of network systems, this is important since a common assumption is that the agents are unaware of the state of the other agents. For example, the addition of a new solar-panel on the power-grid, should not be able to destabilize the entire grid and lead to a power outage, nor should the addition of one vehicle to a platoon noticeably affect the vehicles already in the platoon. All papers in this thesis have considered the scalability of the proposed results. In Paper I, scalable stability and robustness results are proven, concerning the proposed control scheme. In Paper II, scalable performance is analyzed, and in Paper III, bounds which can be used to describe the transient of large-scale systems are derived.

4.2 Future Work

There are many interesting directions for future work. Some of these are listed below.

- Since the serial consensus controller manages to stabilize the n^{th}-order integrator system, it may be possible to consider a Youla-Kucera parametrization of all stabilizing controllers. This can then be used for optimal control design.
- Two methods for implementing the serial consensus controller has been proposed. However, both rely on the agents having access to extra information, either through direct measurements or through message passing. Another approach is to let each agent use a local observer to estimate the relative states. Further investigations into this approach would be of great interest.
- In Paper II, a transient bound for the serial consensus was proven for the case when the same graph Laplacian was used in both factors. This is only a subset of all possible serial consensus systems. It may be possible to utilize the input-output pseudospectra to derive bounds for more complex combinations of serial consensus systems, for instance when the graph Laplacians are not necessarily the same.
- In Paper I and II, the stability, robustness and performance of the serial consensus have been considered. The steady-state behavior of the system has not yet been investigated, but is important to consider.
- Robustness towards time-delays and time-varying graphs has been studied for the conventional consensus. This would also be interesting to study for the serial consensus.
- As is, the robustness results of Paper I assumes the graph Laplacians to be symmetric. Further investigations of the robustness properties of non-symmetric graph Laplacians would be of interest.

Bibliography

Abolfazli, E., B. Besselink, and T. Charalambous (2023). “Minimum time headway in platooning systems under the mpf topology for different wireless communication scenario”. *IEEE Transactions on Intelligent Transportation Systems* **24**:4, pp. 4377–4390.

Andreasson, M., D. V. Dimarogonas, H. Sandberg, and K. H. Johansson (2014). “Distributed control of networked dynamical systems: static feedback, integral action and consensus”. *IEEE Transactions on Automatic Control* **59**:7, pp. 1750–1764.

Bamieh, B., M. R. Jovanovic, P. Mitra, and S. Patterson (2012). “Coherence in large-scale networks: dimension-dependent limitations of local feedback”. *IEEE Transactions on Automatic Control* **57**:9, pp. 2235–2249.

Barooah, P., P. G. Mehta, and J. P. Hespanha (2009). “Mistuning-based control design to improve closed-loop stability margin of vehicular platoons”. *IEEE Transactions on Automatic Control* **54**:9, pp. 2100–2113.

Besselink, B. and S. Knorn (2018). “Scalable input-to-state stability for performance analysis of large-scale networks”. *IEEE Control Systems Letters* **2**:3, pp. 507–512.

Darbha, S., S. Konduri, and P. R. Pagilla (2019). “Benefits of v2v communication for autonomous and connected vehicles”. *IEEE Transactions on Intelligent Transportation Systems* **20**:5, pp. 1954–1963.

Feng, S., Y. Zhang, S. E. Li, Z. Cao, H. X. Liu, and L. Li (2019). “String stability for vehicular platoon control: definitions and analysis methods”. *Annual Reviews in Control* **47**, pp. 81–97.

Gunter, G., D. Gloudemans, R. E. Stern, S. McQuade, R. Bhadani, M. Bunting, M. L. Delle Monache, R. Lysecky, B. Seibold, J. Sprinkle, B. Piccoli, and D. B. Work (2021). “Are commercially implemented adaptive cruise control systems string stable?” *IEEE Transactions on Intelligent Transportation Systems* **22**:11, pp. 6992–7003.

Hansson, J., A. Govaert, R. Pates, E. Tegling, and K. Soltesz (2022). "Limitations of time-delayed case isolation in heterogeneous sir models". In: *2022 American Control Conference*, pp. 2994–2999.

Hansson, J., M. Svensson, A. Theorin, E. Tegling, K. Soltesz, T. Hägglund, and K. J. Åström (2021). "Next generation relay autotuners – analysis and implementation". In: *2021 IEEE Conference on Control Technology and Applications*, pp. 1075–1082.

Hao, H. and P. Barooah (2013). "Stability and robustness of large platoons of vehicles with double-integrator models and nearest neighbor interaction". *International Journal of Robust and Nonlinear Control* **23**:18, pp. 2097–2122.

Hendrickx, J. M. and S. Martin (2017). "Open multi-agent systems: gossiping with random arrivals and departures". In: *2017 IEEE 56th Annual Conference on Decision and Control*, pp. 763–768.

Herman, I., S. Knorn, and A. Ahlén (2017). "Disturbance scaling in bidirectional vehicle platoons with different asymmetry in position and velocity coupling". *Automatica* **82**, pp. 13–20.

Jensen, E. and B. Bamieh (2022). *On structured-closed-loop versus structured-controller design: the case of relative measurement feedback*. arXiv: `2008.11291 [eess.SY]`.

Jiang, F., L. Wang, and Y. Jia (2009). "Consensus in leaderless networks of high-order-integrator agents". In: *2009 American Control Conference*, pp. 4458–4463.

Patterson, S. and B. Bamieh (2014). "Consensus and coherence in fractal networks". *IEEE Transactions on Control of Network Systems* **1**:4, pp. 338–348.

Radmanesh, A., A. Naghash, and A. Mohamadifard (2017). "Optimal distributed control of multi agents: generalization of consensus algorithms for high-order state derivatives of siso and mimo systems". In: *2017 3rd International Conference on Control, Automation and Robotics (ICCAR)*, pp. 606–611.

Ren, W., R. W. Beard, and E. M. Atkins (2007a). "Information consensus in multivehicle cooperative control". *IEEE Control Systems Magazine* **27**:2, pp. 71–82.

Ren, W., K. L. Moore, and Y. Chen (2007b). "High-Order and Model Reference Consensus Algorithms in Cooperative Control of MultiVehicle Systems". *Journal of Dynamic Systems, Measurement, and Control* **129**:5, pp. 678–688.

Rezaee, H. and F. Abdollahi (2015). "Average consensus over high-order multiagent systems". *IEEE Transactions on Automatic Control* **60**:11, pp. 3047–3052.

Seiler, P., A. Pant, and K. Hedrick (2004). "Disturbance propagation in vehicle strings". *IEEE Transactions on Automatic Control* **49**:10, pp. 1835–1842.

Siami, M. and N. Motee (2016). "Fundamental limits and tradeoffs on disturbance propagation in linear dynamical networks". *IEEE Transactions on Automatic Control* **61**:12, pp. 4055–4062.

Stüdli, S., M. Seron, and R. Middleton (2017). “From vehicular platoons to general networked systems: string stability and related concepts”. *Annual Reviews in Control* **44**, pp. 157–172.

Swaroop, D. and J. Hedrick (1996). “String stability of interconnected systems”. *IEEE Transactions on Automatic Control* **41**:3, pp. 349–357.

Tegling, E. (2018). *Fundamental Limitations of Distributed Feedback Control in Large-Scale Networks*. PhD thesis. KTH.

Tegling, E., B. Bamieh, and H. Sandberg (2023). “Scale fragilities in localized consensus dynamics”. *Automatica* **153**, p. 111046.

Willems, J. (1976). “Lyapunov functions for diagonally dominant systems”. *Automatica* **12**:5, pp. 519–523.

Young, G. F., L. Scardovi, and N. E. Leonard (2010). “Robustness of noisy consensus dynamics with directed communication”. In: *Proceedings of the 2010 American Control Conference*, pp. 6312–6317.

Paper I

A closed-loop design for scalable high-order consensus

Jonas Hansson Emma Tegling

Abstract

This paper studies the problem of coordinating a group of n^{th}-order integrator systems. As for the well-studied conventional consensus problem, we consider linear and distributed control with only local and relative measurements. We propose a closed-loop dynamic that we call *serial consensus* and prove it achieves n^{th} order consensus regardless of model order and underlying network graph. This alleviates an important scalability limitation in conventional consensus dynamics of order $n \geq 2$, whereby they may lose stability if the underlying network grows. The distributed control law which achieves the desired closed loop dynamics is shown to be localized and obey the limitation to relative state measurements. Furthermore, through use of the small-gain theorem, the serial consensus system is shown to be robust to both model and feedback uncertainties. We illustrate the theoretical results through examples.

The authors are with the Department of Automatic Control and the ELLIIT Strategic Research Area at Lund University, Lund, Sweden.

This work was partially funded by Wallenberg AI, Autonomous Systems and Software Program (WASP) funded by the Knut and Alice Wallenberg Foundation and the Swedish Research Council through Grant 2019-00691.

1. Introduction

Properties of dynamical systems over networks have been a subject of significant research over the last two decades. A problem of interest the coordination of agents in a network through localized feedback, leading to the prototypical distributed consensus dynamics, studied early on by [Fax and Murray, 2004; Olfati-Saber and Murray, 2004; Jadbabaie et al., 2003]. Over the years, it has become clear that the structural constrains imposed by the network topology in consensus problems often lead to fundamentally poor dynamic behaviors in large networks. This concerns controllability [Pasqualetti et al., 2014], performance [Bamieh et al., 2012; Siami and Motee, 2016] and disturbance propagation [Swaroop and Hedrick, 1996; Seiler et al., 2004], but, as recently highlighted in [Tegling et al., 2023], also stability. The poor stability properties characterized in earlier work [Tegling et al., 2023] (which motivate the present work) apply to higher-order consensus, where the local dynamics of each agent is modeled as an nth order integrator, with $n \geq 2$, and the control is a weighted average of neighbors' relative states. This is a theoretical generalization of first-order consensus [Jiang et al., 2009], but is also relevant in practice. For example, a model where $n = 3$ and thus has consensus in position, velocity and acceleration, can capture flocking behaviors [W. Ren et al., 2006].

More specifically, [Tegling et al., 2023] shows that conventional high-order consensus ($n \geq 3$) is not *scalably stable* for many growing graph structures. When the network grows beyond a certain size, stability is lost. The same holds for second-order consensus ($n = 2$) in, for example, directed ring graphs, as also described in [Stüdli et al., 2017]. To address this lack of scalable stability we propose an alternative generalization of the first-order consensus dynamics, which we prove achieves scalable stability for any model order n.

To illustrate our proposed controller, consider the conventional second-order consensus system where the controller $u(t) = -L_1\dot{x}(t) - L_2x(t) + u_{\text{ref}}(t)$, with $L_{1,2}$ being weighted graph Laplacians, is used to achieve the closed loop

$$\ddot{x}(t) = -L_2\dot{x}(t) - L_1x + u_{\text{ref}}(t). \tag{1}$$

While for first-order consensus ($\dot{x} = Lx + u_{\text{ref}}(t)$), a sufficient condition for convergence to consensus is that the graph underlying the graph Laplacian L contains a connected spanning tree. However, this no longer suffices when $n \geq 2$ as in (1). Therefore, we instead propose the following controller $u(t) = -(L_1 + L_2)\dot{x}(t) - L_1L_2x(t) + u_{\text{ref}}(t)$. The reason for this choice of controller is best illustrated by considering the resulting closed loop in the Laplace domain:

$$(sI+L_1)(sI+L_2)X(s) = U_{\text{ref}}. \quad (2)$$

For this system, like for the first-order case, it is sufficient that the graphs underlying L_1 and L_2 contain a connected spanning tree for the system to eventually coordinate in both x and its derivative $\dot{x}$ (regardless of network size!). This closed loop system, which we will call *serial consensus*, thus mimics one core property of the standard consensus protocol, and can also be generalized to any order n.

The main results of this paper are proofs of some key properties of the proposed n^{th}-order serial consensus. The controller is proven to remain localized (within an n-hop neighborhood) and implementable through relative measurements. We also prove that the closed loop will achieve consensus in all n states. Furthermore, we study the robustness of the proposed closed loop and show that the system will still coordinate when subject to unstructured uncertainty. The beneficial properties of the form (2) (generalized to any order n) are thus not contingent on an idealized implementation.

The remainder of this paper is organized as follows. We first introduce the n^{th} order consensus model and define our choice of control structure. Then the serial consensus system is defined and motivated. In Sec. 3 we provide proofs for the stability and robustness of the serial consensus system. Our main results are then illustrated through examples in Sec. 4. Lastly, we provide our Conclusions in Sec. 5.

2. Problem Setup

We start by introducing some graph theory before introducing the general n^{th} order consensus problem for which we propose the new serial consensus setup. We discuss its properties and then end with some useful definitions.

2.1 Network model and definitions

Let $\mathcal{G} = \{\mathcal{V}, \mathcal{E}\}$ denote a graph of size $N = |\mathcal{V}|$. The set $\mathcal{E} \subset \mathcal{V} \times \mathcal{V}$ denotes the set of edges. The graph can be equivalently represented by the adjacency matrix $W \in \mathbb{R}^{N \times N}$ where $w_{i,j} > 0 \iff (j,i) \in \mathcal{E}$. The graph is called *undirected* if $W = W^T$. The graph contains a *connected spanning tree* if for some $i \in \mathcal{V}$ there is a path from i to any other vertex $j \in \mathcal{V}$.

Associated with a weighted graph we have the weighted graph Laplacian L defined as

$$[L]_{i,j} = \begin{cases} -w_{i,j}, & \text{if } i \neq j \\ \sum_{k \neq i} w_{i,k}, & \text{if } i = j \end{cases}$$

Under the condition that that the graph generating the graph Laplacian contains a connected spanning tree, L will have a simple and unique eigenvalue at 0 and the remaining eigenvalues will lie strictly in the right half plane (RHP).

We will also consider networks with a growing number of nodes. With $\mathcal{G}_N$ we denote a graph in a family $\{\mathcal{G}_N\}$, where N is the size of the growing network.

We will denote the space of all proper, real rational, and stable transfer matrices $\mathcal{RH}_\infty$ and denote the $\mathcal{H}_\infty$ norm as $\|\cdot\|_{\mathcal{H}_\infty}$ following the notation in [Zhou and Doyle, 1998].

2.2 n^{th} order consensus

Let the system be modeled as N agents with identical n^{th} order integrator dynamics, i.e.

$$\frac{\mathrm{d}^n x_i(t)}{\mathrm{d}t^n} = u_i(t), \tag{3}$$

for all $i \in \mathcal{V}$. We will use the convention $x_i^{(0)}(t) = x_i(t)$ and $x_i^{(k)}(t) = \frac{\mathrm{d}^k}{\mathrm{d}t^k} x_i(t)$ to denote time derivatives. When clear we may omit the time argument for brevity.

In this paper we will consider the problem of synchronizing the agents and thus achieve a state of consensus.

Definition 1 (n^{th} order consensus) *The multi-agent system (3) is said to achieve (n^{th} order) consensus if* $\lim_{t\to\infty} |x_i^{(k)}(t) - x_j^{(k)}(t)| = 0$*, for all* $i, j \in \mathcal{V}$ *and* $k \in \{0, 1 \ldots, n-1\}$.

2.3 Control structure

A linear state feedback controller of (3) can be written as

$$u(t) = u_{\text{ref}}(t) - \sum_{k=0}^{n-1} A_k x^{(k)}(t). \tag{4}$$

Where $u_{\text{ref}}(t) \in \mathbb{R}^N$ is a feedforward term and $A_k \in \mathbb{R}^{N\times N}$ represent the feedback of the k^{th} derivative. We will restrict this class of controllers in three ways. The controllers

i) can only use *relative* feedback;

ii) have a limited gain;

iii) and depend on the local neighborhood of each agent.

The limitation to relative feedback translates to the condition $A_k \mathbf{1}_N = 0$ for all k, while a limited gain can be encoded by demanding that $\|A_k\|_\infty \le c$. To capture the notion of locality, consider the adjacency matrix W representing the communication and measurement structure, which we here assume to be the same. That is, if $W_{i,j} = 1$, then agent i can directly receive or measure the relative distance to agent j. Next, consider the non-negative matrix W^q. This matrix has the property that $[W^q]_{i,j} \neq 0$ if and only if there is a path of length q from agent j to agent i. Thus, if we want the controller to only depend on information that is at most q steps away from each agent the following implication should hold: $\sum_{k=0}^{q} W_{i,j}^{k} = 0 \implies [A_k]_{i,j} = 0$. Putting all the conditions together gives us a family of controllers that we will consider in this paper:

DEFINITION 2 (q-STEP IMPLEMENTABLE RELATIVE FEEDBACK) A relative feedback controller of the form (4) is q-step implementable with respect to the adjacency matrix W and gain $c > 0$ if $A_k \in \mathcal{A}^q(W,c)$ for all k, where

$$\mathcal{A}^q(W,c) = \left\{ A \;\middle|\; \begin{matrix} \left[\sum_{k=0}^{q} W^k\right]_{i,j} = 0 \implies A_{i,j} = 0, \\ A\mathbf{1}_N = 0,\ \|A\|_\infty \le c \end{matrix} \right\}.$$

The conventional controller for achieving n^{th} order consensus can be realized as (4) where each A_k is given by a graph Laplacian, e.g. $A_k = L_k \in \mathcal{A}^1(W,c)$. In many cases these are also assumed to be the same such that $L_k = p_k L$ for some graph Laplacian L and constants $p_k > 0$.

2.4 A Novel Design: Serial Consensus

We propose the following controller of (3), expressed in the Laplace domain, to achieve n^{th} order consensus

$$U(s) = U_{\text{ref}}(s) + \left(s^n I - \prod_{k=1}^{n} (sI + L_k) \right) X(s), \tag{5}$$

where L_k are graph Laplacians and U_{ref} is the transformed reference signal. In this case, it is more instructive to consider the closed-loop dynamics, which take the following form:

DEFINITION 3 (n^{TH} ORDER SERIAL CONSENSUS SYSTEM) For all $k \in \{1,2\ldots,n\}$, let L_k be a weighted and directed graph Laplacian. The n^{th}-order serial consensus system is then

$$\left(\prod_{k=1}^{n} (sI + L_k) \right) X(s) = U_{\text{ref}}(s). \tag{6}$$

We call this form serial consensus because the same closed loop dynamics can also be achieved by interconnecting n first-order consensus systems in a series. The closed-loop dynamics in (6) can also be transformed to state-space form by introducing the alternative variables Ξ_k with the corresponding states ξ_k. These relate to X through $\Xi_1 = X(s)$, $\Xi_k = (sI + L_{k-1})\Xi_{k-1}$ for $k \in \{2,\ldots,n-1\}$, and $s\Xi_n = -L_n\Xi_n + U_{\text{ref}}$.

This leads to the following continuous-time state-space representation

$$\begin{bmatrix} \dot{\xi}_1 \\ \dot{\xi}_2 \\ \vdots \\ \dot{\xi}_{n-1} \\ \dot{\xi}_n \end{bmatrix} = \underbrace{\begin{bmatrix} -L_1 & I & & \\ & -L_2 & \ddots & \\ & & \ddots & I \\ & & & -L_n \end{bmatrix}}_{A} \begin{bmatrix} \xi_1 \\ \xi_2 \\ \vdots \\ \xi_{n-1} \\ \xi_n \end{bmatrix} + \begin{bmatrix} 0 \\ 0 \\ \vdots \\ 0 \\ u_{\text{ref}} \end{bmatrix} \tag{7}$$

The serial consensus form has several advantages, which will be the focus of the paper. First, however, we show that it satisfies the constraints we impose on the controller, as given by Definition 2. In other words, we will discuss how the closed-loop structure in (6) can be implemented on a network.

When analysing the serial consensus controller of (5) we will make use of the following assumption on the graph structure.

Assumption A1 (Connected spanning tree) All graphs underlying the graph Laplacians L_k contain a connected spanning tree.

2.5 Implementing Serial consensus

The following proposition ensures that the serial consensus system can be achieved by controlling the n^{th} order integrator system (3) with an n-step implementable relative feedback controller as defined in Definition 2.

Proposition 1 Consider the n^{th}-order serial consensus as defined in (6). If each $L_k \in \mathcal{A}^1(W,c)$ for some constant c and adjacency matrix W, then the controller in (5) is an n-step implementable relative feedback controller with respect to W and a finite gain c'.

To prove this proposition we first need the following two lemmas whose proofs are provided in Appendix A.

Lemma 2 If $A_1 \in \mathcal{A}^{q_1}(W,c_1)$ and $A_2 \in \mathcal{A}^{q_2}(W,c_2)$ then the sum $(A_1+A_2) \in \mathcal{A}^{\max(q_1,q_2)}(W,c_1+c_2)$

Lemma 3 Let $A_1 \in \mathcal{A}^{q_1}(W,c_1)$ and $A_2 \in \mathcal{A}^{q_2}(W,c_2)$ then the product $(A_1A_2) \in \mathcal{A}^{q_1+q_2}(W,c_1c_2)$

Now we can prove *Proposition* 1.

Proof. The serial consensus controller can be expanded to the matrix polynomial

$$\begin{aligned} U(s) &= U_{\text{ref}}(s) + \left(s^n I - \prod_{k=1}^{n} (sI + L_k) \right) X(s) \\ &= U_{\text{ref}}(s) + \left((s^n - s^n) I - \sum_{k=0}^{n-1} s^k A_k \right) X(s), \end{aligned}$$

for some matrices A_k. To show the proposition, we need to show that $A_k \in \mathcal{A}^q(W, c')$ for all $k = 0, \dots, n-1$, with $q \le n$ and $c' < \infty$. Let

$$\mathcal{I}_k = \{\alpha \mid |\alpha| = n-k,\ \alpha \subset \{1, 2, \dots, n\}, \\ i < j \implies \alpha(i) < \alpha(j)\}$$

denote all the ordered subsets of the range $[1, n]$ with size $n-k$. Then

$$A_k = \sum_{\alpha \in \mathcal{I}_k} \prod_{j \in \alpha} L_j, \text{ for all } k \in [0, n-1].$$

Since all $\alpha \in \mathcal{I}_k$ has $n-k$ elements we can show that $\prod_{j \in \alpha} L_j = B_\alpha \in \mathcal{A}^{n-k}(W, c^{n-k})$ by applying Lemma 3 recursively. Now we have a sum

$$A_k = \sum_{\alpha \in \mathcal{I}_k} B_\alpha$$

The number of ordered subsets of the range $[1, n]$ with size $n-k$ is given by the binomial coefficients and therefore the size of $|\mathcal{I}_k| = \binom{n}{n-k}$. Applying Lemma 2 recursively shows that $A_k \in \mathcal{A}^{n-k}(W, \binom{n}{n-k} c^{n-k})$. Clearly, we have that $n-k \le n$ and $\binom{n}{n-k} c^{n-k} \le \binom{n}{\lceil n/2 \rceil} \max(c, c^n) < \infty$ for all k. Let $c' = \binom{n}{\lceil n/2 \rceil} \max(c, c^n)$ and then we have that $A_k \in \mathcal{A}^n(W, c')$ for all k. □

Example 1 For clarity let us consider the controller for the case $n = 3$. Then the controller is

$$\begin{aligned} U(s) &= U_{\text{ref}}(s) + \left(s^3 I - \prod_{k=1}^{3} (sI + L_k) \right) X(s) \\ &= U_{\text{ref}}(s) - \left(s^2 (L_1 + L_2 + L_3) + s(L_1 L_2 + L_1 L_3 + L_2 L_3) + L_1 L_2 L_3 \right) X(s) \end{aligned}$$

Here, $A_0 = L_1 L_2 L_3$, $A_1 = L_1 L_2 + L_1 L_3 + L_2 L_3$, and $A_2 = L_1 L_2 L_3$. The proposition asserts that if L_1, L_2, and L_3 share a sparsity pattern and have bounded gains, then the resulting controller gains A_0, A_1, and A_2 will be sparse and have bounded gains.

2.6 Scalable stability

Coordinating a multi-agent system is inherently a decentralized problem where the goal for each agent is to coordinate with its nearest neighbors. However when the controllers only depend on local measurements there is a possibility that controllers that manage to coordinate N agents stop stabilizing as the number of agents increases. In [Tegling et al., 2023] it was shown that for the 3^{rd} and higher order consensus problem with controller $A_k = a_k L_N$ in (4), the closed loop system will become unstable if the algebraic connectivity $\lambda_2(L_N) \to 0$ as $N \to \infty$. This motivates the notion of *Scalable stability*

DEFINITION 4 (SCALABLE STABILITY [TEGLING ET AL., 2023, DEF. 2.1]) A consensus control design is scalably stable if the resulting closed-loop system achieves consensus over any graph in the family $\{\mathcal{G}_N\}$.

3. Main Results

Our main contribution is two-fold. First we show the serial consensus achieves scalable stability and then we show that the implementation is robust to two classes of perturbations

3.1 Scalable stability

THEOREM 4
Consider the n^{th} order serial consensus system as defined in Definition 3 under Assumption A1 and with $U_{\text{ref}} \in \mathcal{RH}_\infty$. Then the closed loop dynamics have the following properties:

(i) The poles of (6) are given by the union of the eigenvalues of $-L_k$.

(ii) The solution achieves n^{th} order consensus.

Proof. i Any square matrix can be unitarily transformed to upper triangular form by the Schur traingularization theorem. Let $U_k L_k U_k^H = T_k$ be upper triangular. Then the block diagonal matrix $U = \text{diag}(U_1, U_2, \ldots U_n)$ is a unitary matrix that upper triangularizes A in (7). For any triangular matrix the eigenvalues lie on the diagonal and this will be the eigenvalues of each $-L_k$.

(ii) First, consider the closed loop dynamics of (6) which will be

$$X(s) = \left(\prod_{k=n}^{1} (sI + L_k)^{-1} \right) U_{\text{ref}}(s).$$

Since, U_{ref} is stable, we know that the limit $\lim_{s \to 0} U_{\text{ref}}(s) = U_{\text{ref}}(0)$ exists. To prove that the system achieves n^{th} order consensus we want to show that

$$\lim_{t \to \infty} y(t) = \lim_{s \to 0} C(s) X(s) = 0$$

for some transfer matrix $C(s)$, which encodes the consensus states. But since the reference dependence is only related to $U_{\text{ref}}(0)$, we can simplify the problem to only consider impulse responses. But the impulse response has the same transfer function as the initial value response where $\xi_n(0) = U_{\text{ref}}(0)$. Therefore, WLOG, assume that $U_{\text{ref}}(s) = 0$ and an arbitrary initial condition

$$\xi(0) = [\xi_1(0)^T, \xi_2^T, \ldots, \xi_n(0)^T]^T.$$

The solution of (7) is given by $\exp(At)\xi(0) = S\exp(J(A)t)S^{-1}\xi(0)$ where $J(A)$ is the Jordan normal form of A and S is an invertible matrix. From i and the diagonal dominance of the graph Laplacians we know that all eigenvalues of A lie in the left half plane. By Assumption A1 it follows that the zero eigenvalue for each L_k is simple. Now we prove that these n zero eigenvalues form a Jordan block of size n. Let e_k denote the k^{th} 1-block vector, e.g. $\mathbf{e}_1 = \begin{bmatrix}\mathbf{1}_N^T & 0_N & \ldots & 0_N\end{bmatrix}^T$ and $e_2 = \begin{bmatrix}0_N & \mathbf{1}_N^T & 0_N & \ldots & 0_N\end{bmatrix}^T$. Then e_1 is an eigenvector since $A\mathbf{e}_1 = 0$. For $k \in \{2, 3\ldots, n\}$ we have $Ae_k = e_{k-1}$ which implies that $A^k e_k = 0$. This shows that there is a Jordan block of size n with an invariant subspace spanned by the vectors e_k. Since all other eigenvectors make up an asymptotically stable invariant subspace, it follows that $\xi(t)$ will converge towards a solution in $\text{span}(e_1, e_2 \ldots, e_n)$ and thus $\lim_{t\to\infty} \xi_k(t) = \alpha_k(t)\mathbf{1}_N$. Now, since $x(t) = \xi_1(t)$, it follows that $\lim_{t\to\infty} x(t) = \alpha_1(t)\mathbf{1}_N$, and furthermore, since

$$\dot{\xi}_k = -L_k\xi_k + \xi_{k+1} \to \xi_{k+1} \text{ as } t \to \infty$$

for $k \in \{1, \ldots, n-1\}$, it follows that $\lim_{t\to\infty} x^{(k)}(t) = \alpha_{k+1}(t)1_N$ which shows that the system achieves n^{th} order consensus. □

This proposition shows that the stability of the consensus for the n^{th} order serial consensus can be reduced to verifying that the n first-order consensus systems $\dot{x} = -L_k x$ achieve consensus. This is equivalent to determining whether the graphs underlying each L_k contains a connected spanning tree. This result together with *Proposition* 1 shows that n^{th} order consensus can be achieved with a local relative feedback controller with finite gain and thus achieve scalable stability. This result can be compared with [Tegling et al., 2023] where it is shown that the conventional consensus is not scalably stable for any order larger than $n = 3$ if a graph Laplacian with vanishing algebraic connectivity is used. We can summarize this fact in the following corollary:

Corollary 5 *For any n, the controller (5) is scalably stable over any graph family $\{\mathcal{G}_N\}$ that underlies L_k, provided each $\mathcal{G}_N$ satisfies Assumption A1.*

Remark 1 *Note that, by Theorem 4, scalable stability is achieved also with different graph families underlying each L_k, and $||L_k||_\infty$ are allowed to be arbitrarily small.*

3.2 Robustness of serial consensus

The proposed controller in (5) is a relative state-feedback controller which is designed to ensure that the closed loop system achieves n^{th} order consensus as guaranteed through *Theorem* 4. However, the n^{th} order integrator system may be an idealization of the system and the relative state feedback may need observers to be fully realized, and there could be unmodeled dynamics. These potential sources of errors call for a robust controller. We will now present two theorems, which prove that the serial consensus is robust towards two different types of uncertainties.

Additive perturbation The following theorem asserts that the n^{th} order serial consensus controller can handle additive uncertainties.

Theorem 6
Consider the n^{th} order serial consensus system as defined in Definition 3, under Assumption A1, with $L_k = L$ for all k, and $L = L^T$. Then the perturbed system

$$(sI + L)^n X = U_{\text{ref}} + \left(\sum_{k=0}^{n} \Delta_k s^k L^{n-k} \right) X,$$

where $U_{\text{ref}}, \Delta_k \in \mathcal{RH}_\infty$, achieves n^{th} order consensus if

$$\|\Delta_0\|_{\mathcal{H}_\infty} + \|\Delta_n\|_{\mathcal{H}_\infty} + \sum_{k=1}^{n-1} \|\Delta_k\|_{\mathcal{H}_\infty} \sqrt{\frac{k^k}{n^n}(n-k)^{n-k}} < 1.$$

Proof. First, note that the closed-loop system can be represented by the block diagram in Fig. 1, which in turn can be simplified to Fig. 2. Since U_{ref} is stable we can apply the small-gain theorem which asserts that $U(s)$ (as defined in the figures) will be stable if

$$\|\sum_{k=0}^{n} \Delta_k s^k L^{n-k} (sI + L)^{-n}\|_{\mathcal{H}_\infty} < 1.$$

Applying the triangle inequality and submultiplicativity on the left-hand side (LH) yields

$$LH \le \sum_{k=0}^{n} \|\Delta_k\|_{\mathcal{H}_\infty} \|s^k L^{n-k} (sI + L)^{-n}\|_{\mathcal{H}_\infty} \tag{8}$$

Since L is symmetric, it is possible to unitarily diagonalize it. Let $U = U^H$ denote one such unitary matrix. Then $L = U \Lambda U^H$ where Λ is a non-negative real diagonal matrix.

$$\|s^k L^{n-k} (sI + L)^{-n}\|_{\mathcal{H}_\infty} = \|s^k \Lambda^{n-k} (sI + \Lambda)^{-n}\|_{\mathcal{H}_\infty}.$$

For a diagonal matrix the singular values are given by the absolute value of the diagonal. Let, $\lambda > 0$ be an arbitrary positive constant. The maximum gain for each diagonal can then be calculated through

$$\max_{\omega}\left|\frac{\omega^k\lambda^{n-k}}{(j\omega+\lambda)^n}\right| = \sqrt{\max_{\omega}\frac{\omega^{2k}\lambda^{2n-2k}}{(\omega^2+\lambda^2)^n}}.$$

The latter optimization problem is given by a continuous function and thus the derivative must be 0 at the maximum. Simple calculus shows that the optimum is found at $\omega^2 = \lambda^2 k/(n-k)$ for $k = 0,1,\dots n-1$ and at $\omega = \infty$ for $k = n$. Inserting yields

$$\max_{\omega}\left|\frac{\omega^k\lambda^{n-k}}{(j\omega+\lambda)^n}\right| = \begin{cases}\sqrt{\frac{k^k}{n^n}(n-k)^{n-k}} & \text{if } 0 < k < n\\ 1 & \text{else}\end{cases}$$

Now for the case where $\lambda = 0$. Then we have for $k = 0,\dots,n-1$

$$\max_{\omega}\left|\frac{\omega^k 0^{n-k}}{(j\omega+0)^n}\right| = 0$$

and for $k = n$

$$\max_{\omega}\left|\frac{\omega^n}{(j\omega+0)^n}\right| = 1.$$

This is less restrictive than for $\lambda > 0$ and thus we can use the result for $\lambda > 0$. Plugging this into the upper bound of the LH (8) results in the sought inequality.

Finally, we must ensure that stability of the closed loop in Fig. 2 implies n^{th} order consensus. Since the transfer matrix from u to y in Fig. 1 is stable it follows that $Y(s)$ will be stable. This means that we have shown the following $\lim_{t\to\infty} L^{n-k}x^{(k)}(t) = 0$. By Assumption A1 the 0 eigenvalue of L is unique and therefore 0 is a unique eigenvalue of L^{n-k} too. Subsequently, $\lim_{t\to\infty} x^{(k)}(t) \in \ker(L^{n-k})$. Since $L^{n-k}\mathbf{1}_N = 0$ it follows that $\lim_{t\to\infty} x^{(k)}(t) \in \operatorname{span}(\mathbf{1}_N)$ and that the agents will reach consensus in all the $n-1$ first time derivatives and thus achieve n^{th} order consensus. □

It is worth noting that the norm bound on the uncertainty blocks Δ is independent of the number of agents in the system. Therefore, the serial consensus implementation is *scalably robust* in the sense that it allows equally sized perturbations regardless of network size. This is not the case for localized conventional consensus, following the results in [Tegling et al., 2023].

Multiplicative perturbation It is also possible to see the closed-loop serial consensus system as a series of interconnected first-order systems. Therefore it is also interesting to consider the robustness with respect to the individual factors. The following theorem gives a sufficient condition for the unforced closed loop system to achieve n^{th} order consensus.

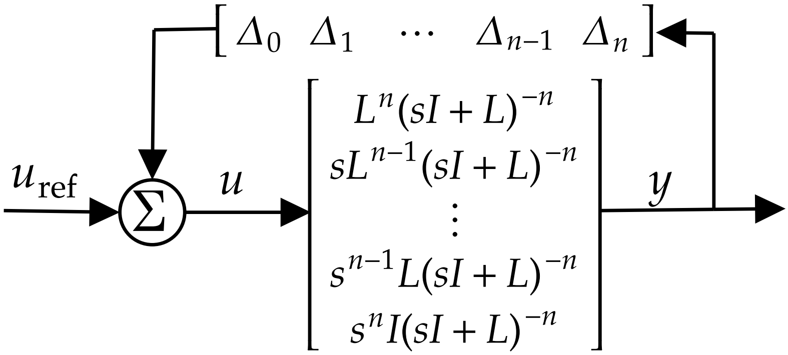

Figure 1. Block diagram illustrating the perturbation model in proof of *Theorem* 6.

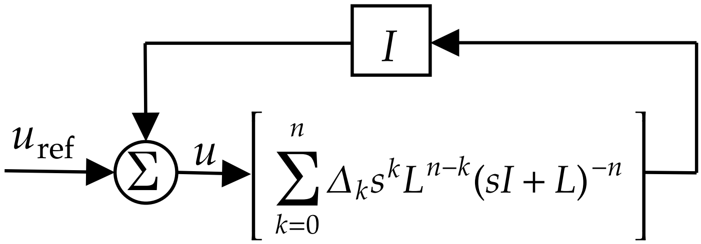

Figure 2. Block diagram illustrating the perturbation model in proof of *Theorem* 6.

THEOREM 7

The following perturbed n^{th} order serial consensus system

$$(sI + s\Delta_0 + (I+\Delta_n)L_n)\prod_{k=1}^{n-1}(sI + (I+\Delta_k)L_k)\,X = U_{\text{ref}}$$

where $U_{\text{ref}}, \Delta_k \in \mathcal{RH}_\infty$ and $L_k = L_k^T$ for $k = 1,\ldots,n$, achieves n^{th} order consensus if

$$\|\Delta_k\|_{\mathcal{H}_\infty} < 1, \textit{ for all } k$$

and

$$\|\Delta_0\|_{\mathcal{H}_\infty} + \|\Delta_n\|_{\mathcal{H}_\infty} < 1.$$

Proof. First, note that we can construct $X(s) = \Xi_1(s)$ and $s\Xi_k = -(I+\Delta_k)L_k\Xi_k + \Xi_{k+1}$ for $k = 1,\ldots,n-1$ and $s(I+\Delta_0)\Xi_n = -(I+\Delta_n)L_n\Xi_n + U_{\text{ref}}$. For Ξ_n we have exactly the 1st order case of *Theorem* 6 and thus $\lim_{t\to\infty}\xi_n(t) = \alpha_n(t)\mathbf{1}_N$ if $\|\Delta_0\|_{\mathcal{H}_\infty} + \|\Delta_n\|_{\mathcal{H}_\infty} < 1$. Consider the following induction hypothesis: if $\Xi_{k+1}(s) = \mathbf{1}_N G_{k+1}(s) +$

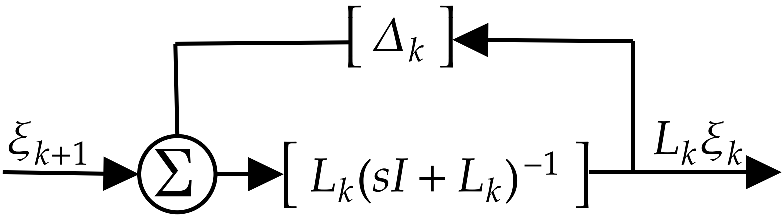

Figure 3. Block diagram illustrating the perturbation model of a general first-order consensus block which is used in the proof of *Theorem* 7.

$H_{k+1}(s)$ where $H_{k+1}(s) \in \mathcal{RH}_\infty$ then $\Xi_k = \mathbf{1}_N G_k(s) + H_k(s)$ for some $H_k(s) \in \mathcal{RH}_\infty$. We have

$$s\Xi_k = -(I+\Delta_k)L_k\Xi_k + \Xi_{k+1}$$

which can be represented by the block diagram Fig. 3. Here, note that

$$L_k(sI+L_k)^{-1}\Xi_{k+1} = (sI+L_k)^{-1}L_k(H_{k+1}(s))$$

and the potentially unstable term of Ξ_{k+1} can be ignored. Reusing a result from the previous proof we have $\|L_k(sI+L_k)^{-1}\|_{\mathcal{H}_\infty} = 1$ and therefore $L_k\Xi_k \in \mathcal{RH}_\infty$ if $\|\Delta_k\|_{\mathcal{H}_\infty} < 1$. Since the 0 eigenvalue of L_k is unique, it follows that $\Xi_k(s) = \mathbf{1}_N G_k(s) + H_k(s)$ with $H_k \in \mathcal{RH}_\infty$ which proves the induction hypothesis since we have already shown the base case $\Xi_n(s) = \mathbf{1}_N G_n(s) + H_n(s)$. Left is to prove that the system will reach n^{th} order consensus. Note that $L_1X(s) = L_1\Xi_1(s)$ is stable and therefore we get through the final value theorem

$$\lim_{t\to\infty} L_1x(t) = \lim_{s\to 0} sL_1\Xi_1(s) = 0.$$

Furthermore, we have for all k: $\lim_{s\to 0} sL_k\Xi_k(s) = 0$. This, combined with $s^2\Xi_k(s) = -(I+\Delta_k)sL_k\Xi_k(s) + s\Xi_{k+1}(s)$ shows that

$$\begin{aligned}\lim_{t\to\infty} L_{k+1}x^{(k)}(t) &= \lim_{s\to 0} s(s^k L_{k+1}X(s)) \\ &= \lim_{s\to 0} sL_{k+1}\Xi_{k+1}(s) = 0\end{aligned}$$

Finally, since the 0 eigenvalues for each L_k are unique with corresponding eigenvector $\mathbf{1}_N$ we see that n^{th} order consensus will be achieved. □

This theorem shows that the n^{th} order serial consensus is robust in its construction.

4. Examples

4.1 2^{nd} order consensus on circular graph

Consider the directed cycle graph, which is represented by the adjacecncy matrix

$$[W]_{i,j} = 1 \text{ iff } i-j = 1 \mod N.$$

The corresponding graph Laplacian L_c is a circulant matrix and therefore, the eigenvalues are known analytically. In particular, the eigenvalue with the second smallest real part is $\lambda_2(L_c) = 1 - \exp(2\pi/N) = 1 - \cos(2\pi/N) - \mathbf{i}\sin(2\pi/N)$. For large N, this eigenvalue can be approximated with a 1st order Taylor approximation, which yields $\lambda_2(L_c) \approx -\mathbf{i}2\pi/N$. This eigenvalue will cause problems when designing a controller using the conventional consensus. To see this, consider the closed loop dynamics

$$s^2 I + 2p_1 s L_c + p_0 L_c = U_{\text{ref}}.$$

The system can be diagonalized and, in particular, two of the poles are given by the equation

$$s^2 + 2p_1\lambda_2(L_c) + p_0\lambda(L_c) = 0.$$

In the case that p_0 and p_1 are designed independently of the network size N, then for sufficiently large N the roots can be approximated as

$$s_p = -p_1\lambda_2 \pm \sqrt{p_1^2\lambda_2^2 - p_0\lambda} \approx \pm(1+\mathbf{i})\sqrt{\frac{\pi p_0}{N}}$$

Since one of these poles will eventually lie in the RHP, it follows that the closed loop system will become unstable when N is sufficiently large, regardless of the choice of p_0 and p_1.

For the serial consensus it suffices to check that all eigenvalues but the unique 0 eigenvalue of L_c lie in the RHP or equivalently if $0 < \text{Re}(\lambda_2(L_C)) = 1 - \cos(2\pi/N)$ which is clearly true for any finite N. Alternatively, it is also sufficient that the underlying graph contains a connected spanning tree.

4.2 3rd order consensus

It has been shown that for $n \geq 3$ it is not possible to achieve scalable stability for any graph family $\{G_N\}$ where the corresponding graph Laplacian L_N has an eigenvalue with vanishing real part as the graph is growing, i.e. if $\lim_{N\to\infty} \text{Re}(\lambda_2(L_N)) = 0$. At least, this is not possible with the conventional consensus control. On the serial consensus form this is no longer a problem. The controller

$$U(s) = U_{\text{ref}} + \left(s^3 I - \prod_{k=1}^{3}(sI + L_N)\right)X(s)$$

will achieve consensus as long as the underlying graphs $\{G_N\}$ all contains a connected spanning tree. To illustrate this, consider the graph defined by $W \in \mathbb{R}^{N\times N}$, the adjacency matrix

$$W_{i,j} = \begin{cases} 1 & \text{if } |i-j| = 1 \text{ and } i \neq 1 \\ 0 & \text{else} \end{cases}.$$

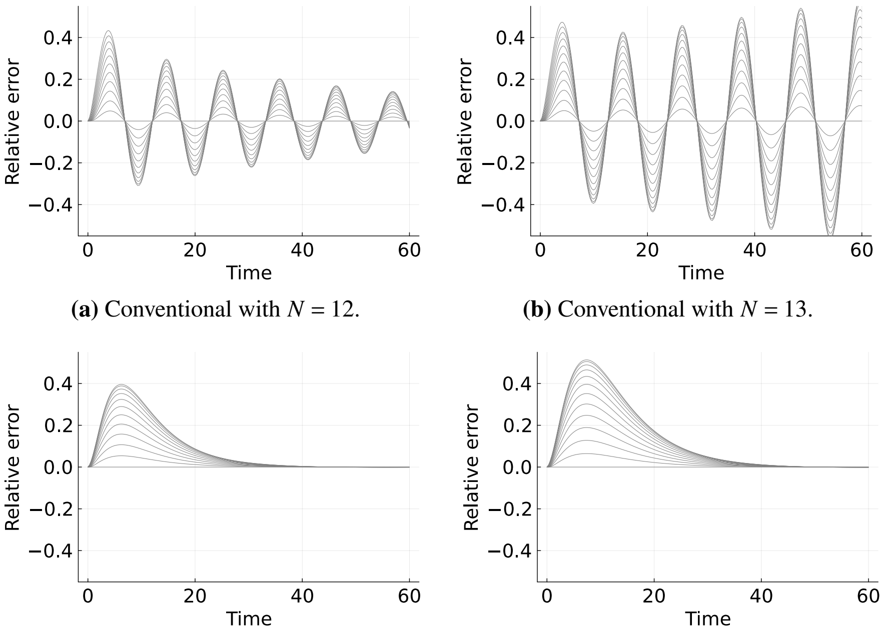

(a) Conventional with $N = 12$.

(b) Conventional with $N = 13$.

(c) Serial with $N = 12$.

(d) Serial with $N = 13$

Figure 4. 3rd order consensus in a chain of vehicles is considered. The plots show the intervehicle relative errors over time when the lead vehicle moves at constant acceleration. Panels (a) and (b) show that the addition of one agent destabilizes the closed loop for the conventional consensus. Panels (c) and (d) illustrate the fact that the serial consensus will remain stable under such agent additions.

This corresponds to a bidirectional string with a leader (Agent 1). Let L be the associated graph Laplacian. It is true that $\lim_{N\to\infty} \lambda_2(L) = 0$ and thus any conventional control design with L will eventually lead to an unstable closed loop. For this example, let the conventional control law be $u(t) = u_{\text{ref}}(t) - 6L\ddot{x} - 4L\dot{x} - 2Lx$ and the serial consensus controller (5) be defined with the same graph Laplacians $L_k = 2kL$. The response to a constant acceleration of the leader is shown in Fig. 4. Here we see that the addition of a 13th agent to the system destabilizes the closed loop for the conventional consensus while the serial consensus only loses some performance.

4.3 Robustness of the 2^{nd} order serial Consensus.

Theorems 6 and 7 show that the serial consensus can be perturbed and still achieve n^{th} order consensus. Now we want to illustrate what the block Δ_k can be. Consider the perturbed 2^{nd} order consensus system in Theorem 6. Writing out all terms we get

$$s^2(I+\Delta_2)X = U_{\text{ref}} - (s(2I+\Delta_1)LX + (I+\Delta_0)L^2X).$$

In this form, the Δ_2 block can be thought of as representing model errors; we may control a system which we model as being N identical double integrator systems but in reality they may differ. This is obviously the case for vehicle platoons, which are often modeled as chains of identical double integrators. Through our theorem we can for instance allow Δ_2 to be a diagonal transfer matrix with elements $[\Delta_2]_{i,i} = \frac{k_i}{T_i s+1}$ where $|k_i| < 1$ and $T_i > 0$ for all i. Then, the closed loop system would remain stable despite the heterogeneous agents. The blocks Δ_1 and Δ_0 are also important. For instance the signals $L^2 x(t)$ and $L\dot{x}(t)$ may not be directly measured but estimated through linear filters. This could be thought of as unmodeled dynamics which these blocks can capture.

If we focus on Theorem 7, then the perturbed model is

$$(s(\Delta_0 + I) + (\Delta_1 + I)L_1)(sI + (\Delta_2 + I)L_2)X = U_{\text{ref}}$$

The theorem only asserts robustness for symmetrical graph Laplacians L_k. However, since Δ_k can also be constant matrices, it is also possible to construct new (asymmetric) graph Laplacians $L'_k = (I + \Delta_k)L_k$ by designing the Δ_k blocks.

5. Conclusion

This work has introduced the n^{th} order serial consensus system which can be seen as a natural generalization of the well-known consensus protocols. The stability of the introduced system can be analysed by considering n regular first order consensus protocol. The proposed controller to achieve n^{th} order serial consensus has been shown to be implementable using relative measurements confined to a local neighborhood of each agent and can therefore be considered a decentralized control scheme. Robustness of the proposed system has also been analyzed. This has been addressed in terms of additive and model perturbations. The analysis showed that the size, measured in the $\mathcal{H}_\infty$ norm, of the allowable uncertainties were independent of the number of agents.

Future and ongoing work includes looking into the performance of the serial consensus and how this relates to string stability. It would also be interesting to look into an implementation where each agent implements an observer to compute their control action.

Appendix A

Here we prove Lemmas 2, 3 which describe how the sparsity pattern of two matrices changes through addition and multiplication.

Proof of Lemma 2

Proof. First, we have $\|A_1 + A_2\|_\infty \leq \|A_1\|_\infty + \|A_2\|_\infty \leq c_1 + c_2$ which follows from the triangle inequality.

For the second part we have $(A_1 + A_2)\mathbf{1}_N = 0 + 0 = 0$.

For the last part, WLOG, suppose that $q_1 \le q_2 = \max(q_1, q_2)$. Since W is a positive matrix, we get

$$0 \le \left(\sum_{k=0}^{q_1} W^k\right)_{i,j} \le \left(\sum_{k=0}^{q_2} W^k\right)_{i,j}.$$

In particular, the following implication follows

$$\left(\sum_{k=0}^{q_2} W^k\right)_{i,j} = 0 \implies \left(\sum_{k=0}^{q_1} W^k\right)_{i,j} \implies [A_1 + A_2]_{i,j} = 0$$

□

Proof of Lemma 3

To prove the result on the product of two matrices, Lemma 3, we need the following three lemmas:

LEMMA 8 Let $A, B \in \mathbb{C}^{N\times N}$ and define $\hat{A}_{i,j} = |A|_{i,j}$ and $\hat{B}_{i,j} = |B|_{i,j}$. If $(AB)_{i,j} \neq 0$ then $(\hat{A}\hat{B})_{i,j} \neq 0$.

Proof. Suppose the statement is false, i.e. $(\hat{A}\hat{B})_{i,j} = 0$ but $(AB)_{i,j} \neq 0$. Then we know that

$$(\hat{A}\hat{B})_{i,j} = \sum_{k=1}^{N} |A_{i,k}||B_{k,j}| = 0,$$

but this implies that at least one of $A_{i,k}$ and $B_{k,j}$ is equal to 0 for all k. But from this it follows that

$$(AB)_{i,j} = \sum_{k=1}^{N} A_{i,k}B_{k,j} = \sum_{k=1}^{N} 0 = 0.$$

This is a contradiction and concludes the proof. □

LEMMA 9 Let $A, A_1, B, B_1 \in \mathbb{R}_+^{N\times N}$. If $(AB)_{i,j} \neq 0$ then $((A + A_1)(B + B_1))_{i,j} \neq 0$.

Proof. Expand the product to get

$$((A + A_1)(B + B_1))_{i,j} = (AB)_{i,j} + (AB_1)_{i,j} + (A_1B)_{i,j} + (A_1B_1)_{i,j} \ge (AB)_{i,j}$$

which followed from the fact that the product of 2 nonnegative matrices is also nonnegative. □

Lemma 10 *Let $A, A_1, B, B_1 \in \mathbb{R}_+^{N\times N}$ be such that $A_{i,j} = 0$ if and only if $A_{1i,j} = 0$, and $B_{i,j} = 0$ if and only if $B_{1i,j} = 0$. Then, $(AB)_{i,j} = 0$ if and only if $(A_1B_1)_{i,j} = 0$.*

Proof. The statement is clearly symmetrical and it is enough to prove sufficiency. Now, if $(AB)_{i,j} = 0$ then we know that

$$\sum_k A_{i,k}B_{k,j} = 0, \implies A_{i,k}B_{k,j} = 0, \; \forall k$$

But this implies that either $A_{i,k} = 0$ or $B_{k,j} = 0$. In turn, this implies that either $(A_1)_{i,k} = 0$ or $(B_1)_{k,j} = 0$. And this leads to

$$(A_1B_1)_{i,j} = \sum_k (A_1)_{i,k}(B_1)_{k,j} = 0$$

□

Now we can prove Lemma 3:

Proof. First, the gain can be bounded as $\|A_1A_2\|_\infty \leq \|A_1\|_\infty\|A_2\|_\infty \leq c_1c_2$ which followed from submultiplicity of the induced norm and from the definition of the sets.

For the second part we have $A_1A_2\mathbf{1}_N = A_1 0 = 0$.

For the last part we have to do slightly more. First replace each element in A_1 and A_2 with its absolute value and denote these B_1 and B_2. Now introduce two non-negative matrices C_1 and C_2 such that $B_1 + C_1 = 0 \iff \sum_{k=0}^{q_1} W^k$ and $B_2 + C_2 = 0 \iff \sum_{k=0}^{q_2} W^k$. Finally note that

$$(\sum_k^{q_1} W^k)(\sum_j^{q_2} W^j) = \sum_k^{q_1+q_2} w_k W^k$$

for some $w_k > 0$. By applying Lemma 10 two times we get that

$$\left[\sum_k^{q_1+q_2} W^k\right]_{i,j} = 0 \implies [(B_1 + C_1)(B_2 + C_2)]_{i,j} = 0$$

Through Lemma 9 we get

$$[(B_1 + C_1)(B_2 + C_2)]_{i,j} = 0 \implies [B_1B_2]_{i,j} = 0$$

And finally applying Lemma 8 results in

$$[B_1B_2]_{i,j} = 0 \implies [A_1A_2]_{i,j} = 0$$

□

Acknowledgement

We want to thank Richard Pates for useful discussions regarding the robustness results.

References

Bamieh, B., M. R. Jovanovic, P. Mitra, and S. Patterson (2012). “Coherence in large-scale networks: dimension-dependent limitations of local feedback”. *IEEE Trans. Autom. Control* **57**:9, pp. 2235–2249.

Fax, J. A. and R. M. Murray (2004). “Information flow and cooperative control of vehicle formations”. *IEEE Trans. Autom. Control* **49**:9, pp. 1465–1476.

Jadbabaie, A., J. Lin, and A. Morse (2003). “Coordination of groups of mobile autonomous agents using nearest neighbor rules”. *IEEE Transactions on Automatic Control* **48**:6, pp. 988–1001.

Jiang, F., L. Wang, and Y. Jia (2009). “Consensus in leaderless networks of high-order-integrator agents”. In: *2009 American Control Conference*, pp. 4458–4463.

Olfati-Saber, R. and R. M. Murray (2004). “Consensus problems in networks of agents with switching topology and time-delays”. *IEEE Trans. Autom. Control* **49**:9, pp. 1520–1533.

Pasqualetti, F., S. Zampieri, and F. Bullo (2014). “Controllability metrics, limitations and algorithms for complex networks”. In: *2014 American Control Conf.* Pp. 3287–3292. DOI: `10.1109/ACC.2014.6858621`.

Seiler, P., A. Pant, and K. Hedrick (2004). “Disturbance propagation in vehicle strings”. *IEEE Transactions on Automatic Control* **49**:10, pp. 1835–1842.

Siami, M. and N. Motee (2016). “Fundamental limits and tradeoffs on disturbance propagation in large-scale dynamical networks”. *IEEE Trans. Autom. Control* **61**:12, pp. 4055–4062.

Stüdli, S., M. M. Seron, and R. H. Middleton (2017). “Vehicular platoons in cyclic interconnections with constant inter-vehicle spacing”. *IFAC-PapersOnLine* **50**:1. 20th IFAC World Congress, pp. 2511–2516.

Swaroop, D. and J. Hedrick (1996). “String stability of interconnected systems”. *IEEE Trans. Autom. Control* **41**:3, pp. 349–357.

Tegling, E., B. Bamieh, and H. Sandberg (2023). “Scale fragilities in localized consensus dynamics”. *Automatica*. To appear. Available: https://arxiv.org/abs/2203.11708.

W. Ren, K. Moore, and Y. Chen (2006). “High-order consensus algorithms in cooperative vehicle systems”. *IEEE International Conf. on Networking, Sensing and Control*, pp. 457–462.

Zhou, K. and J. C. Doyle (1998). *Essentials of robust control*. Vol. 104. Prentice hall Upper Saddle River, NJ.

Paper II

Closed-loop design for scalable performance of vehicular formations

Jonas Hansson   Emma Tegling

Abstract

This paper presents a novel control design for vehicular formations, which is an alternative to the conventional second-order consensus protocol. The design is motivated by the closed-loop system, which we construct as first-order systems connected in series, and is therefore called *serial consensus*. The serial consensus design will guarantee stability of the closed-loop system under the minimum requirement of the underlying communication graph containing a connected spanning tree – which is not true in general for conventional consensus protocol over directed networks. Here, we show that the serial consensus design also gives guarantees on the worst-case transient behavior of the formation, which are independent of the number of vehicles and the underlying graph structure. In particular this shows that the serial consensus design can be used to guarantee string stability of the formation, and is therefore suitable for directed formations. We show that it can be implemented through message passing or measurements to neighbors at most two hops away. The results are illustrated through numerical examples.

In preparation for journal submission.

The authors are with the Department of Automatic Control and the ELLIIT Strategic Research Area at Lund University, Lund, Sweden.

This work was partially funded by Wallenberg AI, Autonomous Systems and Software Program (WASP) funded by the Knut and Alice Wallenberg Foundation and the Swedish Research Council through Grant 2019-00691.

1. Introduction

Network systems emerge in a wide range of applications and engineered networks are, in many cases, becoming increasingly large-scale and complex. Examples include smart power grids, sensor networks, traffic and multi-robot networks, where the coordination of a multitude of interconnected subsystems or agents is a key control problem. The prototypical coordination problem that leads to distributed consensus dynamics was studied early on by [Fax and Murray, 2004; Olfati-Saber and Murray, 2004; Jadbabaie et al., 2003], and the dynamic behaviors of this and related problems has since been the subject of much research. This has made clear that on large scales, consensus-type networks often exhibit poor dynamic behaviors, for example in terms of controllability [Pasqualetti et al., 2014], performance and coherence [Bamieh et al., 2012; Siami and Motee, 2016; Tegling et al., 2019], disturbance propagation [Swaroop and Hedrick, 1996; Seiler et al., 2004; Besselink and Knorn, 2018] and even instability [Tegling et al., 2023]. Motivated by these issues, our work proposes an alternative consensus control design with fundamentally improved scalability properties.

We consider a classical vehicular formation control problem, in which each vehicle in the formation is modeled as a double integrator, whose controller relies on relative state measurements between neighboring vehicles. In the one-dimensional case, this approach can be compactly written on the conventional second-order consensus form

$$\ddot{x}(t) = u(x,t) = -L_1\dot{x}(t) - L_0x(t) + u_{\mathrm{ref}}(t). \tag{1}$$

Here, x is a vector which represents the position of each vehicle, u is a vector of the control inputs, L_1 and L_0 are graph Laplacians, and u_{ref} is a reference control signal. Various assumptions on the feedback structure, here captured by the two graph Laplacians, have been considered over the years. They were assumed to be proportional to each other in the early work [Ren and Atkins, 2007], as well as in more recent analyses [Patterson and Bamieh, 2014; Tegling et al., 2023]. In this case, when the Laplacians capture relative and localized feedback, there are at least three problems with the design (1). First, stability is not guaranteed for all graph Laplacians. For example, the system may be unstable if the Laplacian corresponds to a directed cycle graph. Second, in directed vehicle strings, small errors may amplify throughout the formation and lead to so-called string instability – a topic thoroughly surveyed in [Stüdli et al., 2017b; Feng et al., 2019]. Third, in the case of undirected vehicle formations, the convergence rate of the formation may scale poorly (as $O(1/N^2)$) [Barooah et al., 2009].

A systematic study of the feedback law (1) [Herman et al., 2017] noted that using different Laplacians for the position and velocity dynamics in (1) may drastically improve the performance of the formation. Specifically, symmetric position feedback, i.e. $L_0^T = L_0$, and asymmetric velocity feedback was proposed. However, the stability proof relies on L_0 being perfectly symmetric. In general, these systems are not straightforward to analyze in terms of the underlying topological properties, especially when one factors in scalability, that is, a growth of the network. Several analytic results can, however, be derived under assumptions of spatial invariance, that is, identical agents using the same control and interacation laws.

In this paper we propose a new controller of the vehicle formation: $u(x,t) = -(L_1 + L_2)\dot{x}(t) - L_2L_1x(t) + u_{\text{ref}}(t)$, where L_1 and L_2 are graph Laplacians. The controller is designed to give a particular closed-loop system that we call the second-order *serial consensus system*. The name, as well as the reason for choosing this particular control structure, is easiest seen by considering the closed-loop system in the Laplace domain:

$$(sI + L_2)(sI + L_1)X(s) = U_{\text{ref}}(s).$$

Clearly, the closed-loop system has the same dynamics as two conventional first-order consensus systems put in a series. As for the classical first-order consensus protocol it is true that the consensus equilibrium will be stable as long as the graphs underlying L_1 and L_2 each contain a connected spanning tree. This directly addresses the above mentioned problem of instability in classical second-order consensus. Our main results, however, pertain to the performance of the serial consensus.

It turns out that the serial consensus controller can guarantee a strong notion of (generalized) string stability of the formation. Specifically, given any combination of relative errors $e_p(t) = Lx(t)$, that are defined through a graph Laplacian L, and velocity deviations $e_v(t) = \dot{x}(t) - \mathbf{1}v_{\text{ref}}$, we are able to give bounds on the following form:

$$\sup_{t\geq 0}\left\|\begin{bmatrix} e_p(t) \\ e_v(t)\end{bmatrix}\right\|_\infty \leq \alpha \left\|\begin{bmatrix} e_p(0) \\ e_v(0)\end{bmatrix}\right\|_\infty .$$

Here α is a constant independent of the number of vehicles and the underlying graph structure (that is, it need not be a string). The importance of this result stems from the fact that the bound is in terms of the ℓ^∞-norm. Results of this type has been suggested to be more suitable for large vehicle formations [Feintuch and Francis, 2012; Stüdli et al., 2017a], especially to ensure scalability [Besselink and Knorn, 2018], however typically hard to derive. The result implies that our design addresses the earlier mentioned problems of conventional consensus. Under mild conditions the closed loop will be stable, it can be designed to achieve string stability, and since directed graphs are allowed, the convergence rate can be improved. The cost of this advantage is, in some cases, a requirement for one additional communication step, either through physical measurement or signaling. Such additional signaling has been proposed in a vehicular platooning context in e.g. [Darbha et al., 2019]. We argue, however, that our structure gives greater benefits with a smaller communications overhead.

The remainder of the paper is organized as follows. In Section 2 we introduce the problem setup and the notation used throughout the paper. Here, the serial consensus system is also defined together with some key properties. In Section 3 we present our performance results in the form of a theorem. The results are illustrated in Section 5 through numerical examples. Finally, we conclude the paper in Section 6.

2. Problem Setup

2.1 Definitions and network model

Let $\mathcal{G} = \{\mathcal{V}, \mathcal{E}\}$ denote a graph of size $N = |\mathcal{V}|$ with the edge set $\mathcal{E} \subset \mathcal{V} \times \mathcal{V}$. The graph can be equivalently represented by the weighted adjacency matrix $W \in \mathbb{R}^{N\times N}$ where $w_{i,j} > 0 \iff (i, j) \in \mathcal{E}$. The graph is called *undirected* if $W = W^T$. The graph contains a *connected spanning tree* if for some $i \in \mathcal{V}$ there is a path from i to any other vertex $j \in \mathcal{V}$.

The weighted graph Laplacian L associated to the graph is defined as

$$[L]_{i,j} = \begin{cases} -w_{i,j}, & \text{if } i \neq j \\ \sum_{k\neq i} w_{i,k}, & \text{if } i = j \end{cases}. \tag{2}$$

Under the condition that that the graph generating the graph Laplacian contains a connected spanning tree, L will have a simple and unique eigenvalue at 0 and the remaining eigenvalues will lie strictly in the right half plane (RHP). We will refer to any $N\times N$ matrix that satisfies (2) for some set of weights $w_{i,j}$ as a graph Laplacian.

We will denote the space of all proper, real rational, and stable transfer matrices $\mathcal{RH}_\infty$ and denote the $\mathcal{H}_\infty$-norm as $\|\cdot\|_{\mathcal{H}_\infty}$ following the notation in [Zhou and Doyle, 1998]. By $\|\cdot\|_\infty$, we denote the standard vector norm and its corresponding induced matrix norm i.e. $\|z\|_\infty = \max_k |z_k|$, where $z \in \mathbb{C}^N$ and with $\|M\|_\infty = \sup_{\|x\|_\infty=1} \|Mx\|_\infty$, for $M \in \mathbb{C}^{N\times N}$.

2.2 Vehicle formation model

Consider a simple vehicle formation which consists of N identical double integrator systems, i.e.

$$\frac{\mathrm{d}^2 x_i(t)}{\mathrm{d}t^2} = u_i(x, t), \quad i = 1, \ldots, N, \tag{3}$$

where $x_i(t) \in \mathbb{R}$ The aim is to coordinate the vehicles to keep a fixed spacing and common velocity. This goal is related to the problem of achieving *second order consensus* as defined below.

Definition 5 (Second order consensus) The vehicle formation (3) is said to achieve second order consensus if

$$\lim_{t\to\infty}\left|\frac{\mathrm{d}x_i(t)}{\mathrm{d}t}-\frac{\mathrm{d}x_j(t)}{\mathrm{d}t}\right| = 0 \text{ and } \lim_{t\to\infty}|x_i(t)-x_j(t)| = 0$$

for all $i, j \in \mathcal{V}$.

With our control structure, the desired, fixed intervehicle distances can without loss of generality be set to zero for analysis purposes. This will be clarified in Remark 3.

Remark 2 In this work we only consider a scalar state, that is, longitudinal control. The results can be extended to higher spatial dimensions (see e.g. [Oh et al., 2015] for a survey of approaches), but we omit it here to keep notation simple.

2.3 Control structure

In this work, we will consider linear state feedback controllers of the system (3). Such controllers can be written as

$$u(t) = u_{\text{ref}}(t) - A_1\dot{x}(t) - A_0x(t), \tag{4}$$

where $x = (x_1, x_2, \ldots, x_N)^T \in \mathbb{R}^N$, $u_{\text{ref}}(t) \in \mathbb{R}^N$ is a feedforward term, and $A_0, A_1 \in \mathbb{R}^{N\times N}$ are constant feedback matrices for the position and velocity respectively. In the distributed coordination problem, the controller is further restricted to

i) only use *relative* feedback;

ii) have a bounded gain;

iii) only depend on the local neighborhood of each agent.

These restrictions are captured by considering controllers which are part of the following class.

Definition 6 (q-step implementable relative feedback) The relative state feedback $u = Ax$ is q-step implementable with respect to the adjacency matrix W and gain $c > 0$ if $A \in \mathcal{A}^q(W,c)$, where

$$\mathcal{A}^q(W,c) = \left\{ A \;\middle|\; \begin{array}{c} \left[\sum_{k=0}^{q} W^k\right]_{i,j} = 0 \implies A_{i,j} = 0, \\ A\mathbf{1} = 0,\ \|A\|_\infty \le c \end{array} \right\}.$$

Clearly, the sum of two q-step implementable controllers is also q-step implementable so if both $A_0, A_1 \in \mathcal{A}^q(W,c)$ then the combined controller in (4) will also be q-step implementable. To clarify the concept of q-step implementability, consider the following example.

Example 2 *Consider a vehicle string where each agent can measure the distance to its two neighboring vehicles. This structure can be represented by the adjacency matrix W such that* $[W]_{i,j} = 1 \iff |i-j| = 1$. *and* $W_{i,j} = 0$ *otherwise. Then the sparsity constraint of* $A \in \mathcal{A}^q(W,c)$ *corresponds to the requirement that*

$$|i-j| > q \implies [A]_{i,j} = 0,$$

i.e., that only relative measurements up to the q nearest neighbors are used. One choice of a 1*-step implementable matrix* ($A \in \mathcal{A}^1(W,c)$) *is the graph Laplacian* $A = L$ *while an example of a* 2*-step implementable matrix is* $A = L^2$.

In general, if the adjacency matrix W captures a physical network, then a controller $u = Ax$ with $A \in A^q(W,c)$ means u_i requires signals from Agent i's q-hop neighborhood. This is readily proven; we refer the reader to [Hansson and Tegling, 2023].

A controller that has been widely applied for vehicle formations in the literature is what we will call the *conventional consensus* controller. In this case both $A_0 = L_0$ and $A_1 = L_1$ are chosen to be graph Laplacians and this results in the controller being a 1-step implementable relative-feedback controller. The closed-loop dynamics with this controller are

$$\ddot{x} = -L_1\dot{x} - L_0x + u_{\text{ref}}. \tag{5}$$

This is, however, not the only way to implement a controller satisfying the desired structure. We next propose our alternative approach.

Remark 3 *The analysis of a formation with position offsets can be made on the translated states* $\tilde{x} = x - p - tv_{\text{ref}}\mathbf{1}$ *where* $p \in \mathbb{R}^N$ *is a vector of desired offsets and* v_{ref} *a desired velocity. If the reference control signal is chosen to be* $u_{\text{ref}} = \tilde{u}_{\text{ref}} + A_0p$ *then the closed-loop dynamics in the new states becomes*

$$\ddot{\tilde{x}} = \tilde{u}_{\text{ref}} - A_1\dot{\tilde{x}} - A_0\tilde{x}$$

where the property $A_0\mathbf{1} = A_1\mathbf{1} = 0$ *was used. Thus, the dynamics around any potential offset will be equivalent to the dynamics of x when* $p = 0$ *and* $v_{\text{ref}} = 0$.

2.4 A Novel Design: Serial Consensus

To address the problems of stability, performance, and robustness of interconnected double-integrator systems we propose a controller design which achieves a desired closed loop. Due to its structure, we term it the second order serial consensus system.

Definition 7 (Second order serial consensus system) *Let* L_1 *and* L_2 *be weighted and directed graph Laplacians. The second-order serial consensus system is then*

$$(sI + L_2)(sI + L_1)X(s) = U_{\text{ref}}(s). \tag{6}$$

The system (3) achieves the serial consensus system through the control design

$$u(x,t) = u_{\text{ref}}(t) - (L_2 + L_1)\dot{x}(t) - L_2 L_1 x(t). \tag{7}$$

When analyzing the serial consensus controller of (6) we will make use of the following assumption on the graph structure.

ASSUMPTION A2 (CONNECTED SPANNING TREE) The graphs underlying the graph Laplacians L_1 and L_2 contain a connected spanning tree.

A convenient state-space representation of the serial consensus system is

$$\begin{bmatrix} \dot{\xi}_1 \\ \dot{\xi}_2 \end{bmatrix} = \underbrace{\begin{bmatrix} -L_1 & I \\ 0 & -L_2 \end{bmatrix}}_{A} \begin{bmatrix} \xi_1 \\ \xi_2 \end{bmatrix} + \begin{bmatrix} 0 \\ u_{\text{ref}} \end{bmatrix}. \tag{8}$$

This can be transformed back to x and $\dot{x}$ through the linear transformations

$$\begin{bmatrix} x \\ \dot{x} \end{bmatrix} = \begin{bmatrix} I & 0 \\ -L_1 & I \end{bmatrix} \begin{bmatrix} \xi_1 \\ \xi_2 \end{bmatrix} \text{ and } \begin{bmatrix} \xi_1 \\ \xi_2 \end{bmatrix} = \begin{bmatrix} I & 0 \\ L_1 & I \end{bmatrix} \begin{bmatrix} x \\ \dot{x} \end{bmatrix}$$

One benefit of considering the serial consensus can be understood through the following theorem

THEOREM 11
Consider the second order serial consensus system as defined in Definition 7 under Assumption A2 and with $U_{\text{ref}} \in \mathcal{RH}_\infty$. Then the closed loop dynamics have the following properties:

i) The poles of (6) are given by the union of the eigenvalues of $-L_1$ and $-L_2$.

ii) The solution achieves second order consensus.

The proof, a version of which appeared in [Hansson and Tegling, 2023], is presented in Appendix 6. For the conventional consensus a theorem like this does not exist, since using, e.g., a Laplacian corresponding to a directed cycle can result in an unstable closed loop as noted in [Stüdli et al., 2017b; Tegling et al., 2023]. Serial consensus, on the other hand, can be shown to be robustly stable, see [Hansson and Tegling, 2023] for the robustness criteria.

The serial consensus controller is at worst 2-step implementable as per the following result.

PROPOSITION 12 Consider the second-order serial consensus controller (7). If $L_1, L_2 \in \mathcal{A}^1(W,c)$ for a constant c and adjacency matrix W, then the controller is a 2-step implementable relative feedback controller with respect to W and gain $c' = \max\{2c, c^2\}$.

The proof is found in the Appendix B, which is a version of what appeared in [Hansson and Tegling, 2023]. The actual implementation of the serial consensus will be discussed in further detail after our main results.

2.5 Performance criterion

Motivated by the setting of vehicle formations we introduce the following two errors. First, let the relative position be defined by

$$e_p(t) := d + Lx(t),$$

where the graph $\mathcal{G}_N$ underlying the graph Laplacian L has size N and $d \in \mathbb{R}^N$ is a vector of desired offsets. Second, denote the velocity deviation as

$$e_v(t) := \dot{x}(t) - v_{\text{ref}}\mathbf{1},$$

with $v_{\text{ref}} \in \mathbb{R}$ being the desired vehicle velocity.

The error e_p represents the local relative position errors. This needs to remain small to prevent vehicle collisions. Meanwhile, e_v represents the deviation from the desired velocity. In a vehicle formation this error needs to be small to ensure that speed limits are respected. This should remain true also as the network grows, that is, the errors should be independent of the number of agents N.

Definition 8 (Scalable performance) A formation controller defined over a growing family of graphs that ensures

$$\sup_{t\geq 0}\left\|\begin{bmatrix} e_p(t) \\ e_v(t)\end{bmatrix}\right\|_\infty \leq \alpha \left\|\begin{bmatrix} e_p(0) \\ e_v(0)\end{bmatrix}\right\|_\infty, \tag{9}$$

where α is fixed and independent of N, is said to achieve scalable performance.

Here, the choice of norm is important since the worst-case behavior gets bounded by the initial maximum deviation. We remark that we only consider the initial-value response. While the disturbance amplification scenario also requires careful analysis as discussed in [Besselink and Knorn, 2018], we leave it outside the scope of the present study.

3. Main Results

Here we show that position and velocity errors can be kept small throughout the transient phase. This is achieved through the use of a serial consensus controller which uses measurements based on the underlying network graph. The result is summarized in the following theorem.

Theorem 13
Let $e_p = Lx$ where L is a graph Laplacian. If the system $\ddot{x}(t) = u(t)$ is controlled with

$$u(t) = -(p_1 + p_2)L\dot{x}(t) - p_1 p_2 L^2 x(t),$$

where $p_1, p_2 > 0$ and $p_1 \neq p_2$, then the resulting serial consensus system achieves scalable performance with

$$\alpha = \frac{1}{|p_1 - p_2|}\left(p_1 + p_2 + \max\{2, 2p_1p_2\}\right).$$

Proof. The serial consensus system can be rewritten as

$$\begin{bmatrix}\dot{\xi}_1\\ \dot{\xi}_2\end{bmatrix} = \begin{bmatrix}-p_1L & I\\ 0 & -p_2L\end{bmatrix}\begin{bmatrix}\xi_1\\ \xi_2\end{bmatrix} + \begin{bmatrix}0\\ u_{\text{ref}}\end{bmatrix}.$$

Here $\xi_1 = x$ and $\xi_2 = \dot{x} + p_1Lx$. Since $u_{\text{ref}} = 0$, the initial value problem can be solved directly. This evaluates to

$$\begin{aligned}\xi_1(t) &= e^{-p_1Lt}\xi_1(0) + e^{-p_1Lt}\int_0^t e^{p_1L\tau}e^{-p_2L\tau}\mathrm{d}\tau\xi_2(0)\\ \xi_2(t) &= e^{-p_2Lt}\xi_2(0).\end{aligned}$$

Since p_1L and p_2L obviously commute, it follows that $e^{p_1L\tau}e^{-p_2L\tau} = e^{(p_1-p_2)L\tau}$. By pre-multiplying the first equation with $(p_1 - p_2)L$ and using the property that L commutes with e^{-p_1Lt} we finally get the integrand $(p_1 - p_2)Le^{(p_1-p_2)L\tau} = \frac{\mathrm{d}}{\mathrm{d}t}(e^{(p_1-p_2)L\tau})$. Finally, by applying the Fundamental Theorem of Calculus the equation can be simplified to

$$L\xi_1(t) = e^{-p_1Lt}L\xi_1(0) + \frac{(e^{-p_2Lt} - e^{-p_1Lt})}{p_1 - p_2}\xi_2(0).$$

Now, inserting that $e_p(t) = L\xi_1(t)$, $\dot{x}(t) = \xi_2(t) - p_1e_p(t)$, and $e_v(t) = \dot{x} - v_{\text{ref}}\mathbf{1}$ yields

$$e_p(t) = e^{-p_1Lt}e_p(0) + \frac{e^{-p_2Lt} - e^{-p_1Lt}}{p_1 - p_2}(e_v(t) + v_{\text{ref}}\mathbf{1} + p_1e_p(0)).$$

Next we note that the relation $e^{-Lt}\mathbf{1} = \mathbf{1}$ holds for any graph Laplacian L. In particular, this implies that $(e^{-p_2Lt} - e^{-p_1Lt})\mathbf{1} = 0$. After some simplifications this leads to

$$e_p(t) = \frac{p_1e^{-p_2Lt} - p_2e^{-p_1Lt}}{p_1 - p_2}e_p(0) + \frac{e^{-p_2Lt} - e^{-p_1Lt}}{p_1 - p_2}e_v(0)$$

$$\begin{aligned}e_v(t) &= -p_1e_p(t) + e^{-L_2t}(e_v(0) + p_1e_p(0))\\ &= \frac{p_1p_2\left(e^{-p_1Lt} - e^{-p_2Lt}\right)}{p_1 - p_2}e_p(0) + \frac{p_1e^{-p_1Lt} - p_2e^{-p_2Lt}}{p_1 - p_2}e_v(0).\end{aligned}$$

Taking the induced norm $\|\cdot\|_\infty$ and then applying the triangle inequality yields the following two bounds:

$$\|e_p(t)\|_\infty \leq \frac{p_1+p_2}{|p_1-p_2|}\|e_p(0)\|_\infty + \frac{2}{|p_1-p_2|}\|e_v(0)\|_\infty$$

and

$$\|e_v(t)\|_\infty \leq \frac{2p_1p_2}{|p_1-p_2|}\|e_p(0)\|_\infty + \frac{p_1+p_2}{|p_1-p_2|}\|e_v(0)\|_\infty.$$

Finally, we have that

$$\|e_p\|_\infty, \|e_v\|_\infty \leq \left\|\begin{bmatrix} e_p \\ e_v \end{bmatrix}\right\|_\infty = \max\{\|e_p\|_\infty, \|e_v\|_\infty\}$$

Combining these facts yields

$$\left\|\begin{bmatrix} e_p(t) \\ e_v(t) \end{bmatrix}\right\|_\infty \leq \frac{p_1+p_2+2\max\{1,p_1p_2\}}{|p_1-p_2|}\left\|\begin{bmatrix} e_p(0) \\ e_v(0) \end{bmatrix}\right\|_\infty,$$

which is the definition of scalable performance with α as in the theorem statement.□

REMARK 4 *In the limit when p_1 approaches infinity and p_2 approaches 0 (or vice versa) then the theoretically optimal bound of $\alpha = 1$ is retrieved. For instance, let $p_1 = x$ and $p_2 = 1/x$. Then, for $x > 1$ we get*

$$\lim_{x\to\infty} \alpha(x) = \lim_{x\to\infty} \frac{x+1/x+2}{x-1/x} = 1.$$

In this case the dynamics are essentially reduced to a first order consensus system, which may be desirable. This would however require an unbounded gain.

4. Implementation

The serial consensus protocol has now been shown to have both scalable stability and performance. It turns out that this also holds true for the implementation. In the vehicle formation setting we desire a controller which has a finite gain, uses few measurements, and has a decentralized implementation.

The graphs underlying $L_1 + L_2$ and L_2L_1 must be implemented by the controller. While this requires carefully designed signaling, it is still easy to implement as a controller with finite gain and localized measurements.

4.1 Message passing

One way to implement serial consensus is through message passing. The reason can be explained through the control law which is

$$u = -(L_2+L_1)\dot{x} - L_2L_1x + u_{\text{ref}}.$$

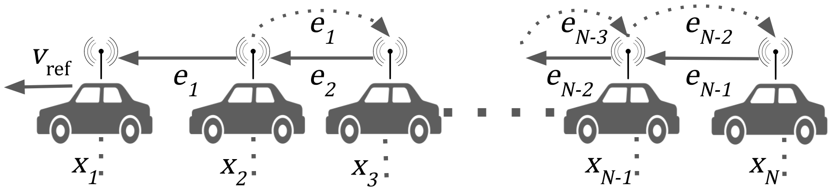

Figure 1. Vehicle platoon with directed measurements and message passing to implement serial consensus.

The velocity feedback will be implementable using only relative measurements from each agent, provided that both L_1 and L_2 are localized graph Laplacians. Message passing is instead needed for the positional feedback. This can be implemented if each agent stores their relative error $e_i = [L_1 x]_i$. Then if each agent can access their out-neighbor's error, then the control signal can be calculated through $L_2 L_1 x = L_2 e$. In the case of a vehicle platoon, the relative distance to the first neighbor can be measured through the use of radar. However, the relative distance to the second neighbor requires an additional signaling layer. That is, if such signaling can be had with the nearest neighbor, then it is implementable in a platoon. This idea of signaling is illustrated in Fig. 1.

4.2 Extended measurements

Using a step of communication is not the only way to implement the serial consensus. Instead, $L_2 L_1$ can be implemented through direct measurements. Indeed, with careful design, it is possible to choose L_2, L_1 so that their product $(L_2 L_1) \in \mathcal{A}^1(W, c)$ and is thus implementable using only relative measurements with immediate neighbors. The following example illustrates this case.

Example 3 Let $W_{\text{undir-path}}$ correspond to the undirected path graph, i.e.

$$(W_{\text{undir-path}})_{i,j} = 1 \iff |i - j| = 1.$$

Furthermore, let $L_{\text{ahead-path}}$ and $L_{\text{behind-path}}$ correspond to the look-ahead and look-behind path graphs, respectively:

$$L_{\text{ahead-path}} = \begin{bmatrix} 0 & 0 & & \\ -1 & 1 & & \\ & \ddots & \ddots & \\ & & -1 & 1 \end{bmatrix} \in \mathcal{A}^1(W_{\text{undir-path}}, 2) \tag{10}$$

and

$$L_{\text{behind-path}} = \begin{bmatrix} 1 & -1 & & \\ & \ddots & \ddots & \\ & & 1 & -1 \\ & & 0 & 0 \end{bmatrix} \in \mathcal{A}^1(W_{\text{undir-path}}, 2). \tag{11}$$

Then, the product of these two matrices will be

$$L_{\text{behind-path}} L_{\text{ahead-path}} = \begin{bmatrix} 1 & -1 & & & & \\ -1 & 2 & -1 & & & \\ & \ddots & \ddots & \ddots & & \\ & & -1 & 2 & -1 & \\ & & & & 0 & 0 \end{bmatrix}.$$

Since the product only requires information from the neighboring states it holds that

$$L_{\text{behind-path}} L_{\text{ahead-path}} \in \mathcal{A}^1(W_{\text{undir-path}}, 4),$$

and the same holds true for $(L_{\text{behind-path}} + L_{\text{ahead-path}})$*. This shows that the serial consensus controller with* $L_2 = L_{\text{behind-path}}$ *and* $L_1 = L_{\text{ahead-path}}$ *would be* 1*-step implementable, and thus only requires local relative feedback.*

On the other hand, if $L_2 L_1 \notin \mathcal{A}^1(W, c)$, then another alternative is to extend the local measurements. It is then sufficient to add measurements to neighbors' neighbors. That is, given $L_1, L_2 \in \mathcal{A}^1(W, c)$, then it holds that the product $(L_2 L_1) \in \mathcal{A}^2(W, c')$, as guaranteed by Proposition 12. The sum will clearly satisfy $(L_2 + L_1) \in \mathcal{A}^1(W, 2c)$.

5. Examples

In this section we will provide three examples which will illustrate our main results and how serial consensus compares to the conventional consensus protocol.

5.1 Scalable stability

EXAMPLE 4 *Consider the uni-directional circular graph structure with the graph Laplacian defined as*

$$(L_{\text{ahead-cycle}})_{ij} = \begin{cases} 1 & \text{if } i = j \\ -1 & \text{if } i = j+1 \pmod{N} \end{cases}.$$

The conventional consensus protocol is then

$$\ddot{x} = -r_1 L_{\text{ahead-cycle}} \dot{x} - r_0 L_{\text{ahead-cycle}} x + u_{\text{ref}}$$

This system is known to be troublesome, since unless q_1 *and* q_0 *are chosen to depend on the number of vehicles N, the closed-loop system will be unstable for large N. Algebraically, this is a consequence of the smallest in magnitude eigenvalues of* $L_{\text{ahead-cycle}}$ *approaching the origin at an angle to the real axis as N grows [Tegling et al., 2023].*

On the other hand, the serial consensus protocol

$$\ddot{x} = -(p_1 + p_2)L_{\text{ahead-cycle}}\dot{x} - p_1 p_2 L^2_{\text{ahead-cycle}} x + u_{\text{ref}}$$

is stable for any N as long as p_1 and p_2 are chosen to be positive, which follows from Theorem 11. Provided $p_1 \neq p_2$, Theorem 13 also predicts that it has scalable performance with respect to the graph Laplacian $L_{\text{ahead-cycle}}$.

A comparison of the transient behavior for the two formations is shown in Fig. 2. The figure shows how the formation that is controlled through the serial consensus protocol is stable and has similar behavior independent of the number of vehicles. Meanwhile, the one controlled with conventional consensus has similar performance for small N but eventually loses stability for large N.

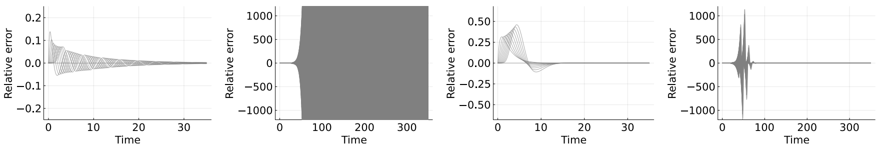

(a) Directed cycle, conventional consensus with $N = 10$. **(b)** Directed cycle, conventional consensus with $N = 100$. **(c)** Directed path, conventional consensus with $N = 10$ **(d)** Directed path, conventional consensus with $N = 100$

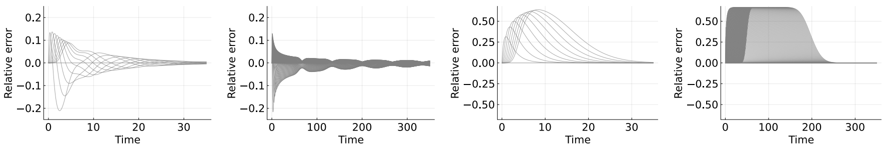

(e) Directed cycle, serial consensus with $N = 10$. **(f)** Directed cycle, serial consensus with $N = 100$. **(g)** Directed path, serial consensus with $N = 10$. **(h)** Directed path, serial consensus with $N = 100$.

Figure 2. Simulation of the initial value response to $x = 0$, $\dot{x}_{i\neq 1}(0) = 0$, and $\dot{x}_1(0) = 1$. For the serial consensus, $p_1 = 2$ and $p_2 = 0.5$ was used and for the conventional $r_1 = 2.5$ and $r_0 = 1$ was used. Different graph structures and number of vehicles N was tested. For each plot the inter-vehicle distances $e_p(t) = L_{\text{ahead-path}}x(t)$ are shown. The conventional consensus system can be seen to degrade with increasing number of vehicles N, while the serial consensus displays scalable stability and performance.

5.2 Scalable performance

Example 5 Here we will illustrate the significant difference in performance between conventional and serial consensus in the case of a directed vehicle string. For this purpose, consider the directed path topology whose graph Laplacian is given by (10). In this case it is easy to verify that the conventional consensus protocol

$$\ddot{x} = -r_1 L_{\text{ahead-path}}\dot{x} - r_0 L_{\text{ahead-path}} x + u_{\text{ref}}$$

will stabilize the vehicle formation for any choice of positive r_1 and r_0. However, the transient behavior will scale poorly independent of the choice of r_1 and r_0 as is illustrated in Fig. 2. The formation under this control is well known to lack string stability [Seiler et al., 2004], that is, disturbances propagate and grow along the string. On the other hand, the serial consensus protocol with

$$\ddot{x} = -(p_1 + p_2)L_{\text{ahead-path}}\dot{x} - p_1 p_2 L^2_{\text{ahead-path}} x + u_{\text{ref}}$$

will have scalable performance with respect to the position error $e_p = d + L_{\text{ahead-path}} x$ and velocity error e_v as long as $p_1 \neq p_2$. This is illustrated in Fig. 2g and Fig. 2h, where the same initial conditions and parameters are used for both consensus protocols. From the figures it is clear that both formations are stable. However, the conventional consensus protocol has a much larger transient than the serial consensus protocol, which will get worse as the number of vehicles increases.

5.3 Different graph Laplacians

EXAMPLE 6 *The conventional consensus design has been shown to have acceptable performance in a vehicle string when different Laplacians are used in the position and velocity feedback [Herman et al., 2017]. In particular, the use of the directed path graph Laplacian for the velocity term (look-ahead) and an undirected path graph Laplacian for the positional term (look-ahead and look-behind), defined as*

$$(L_{\text{undir-path}})_{ij} = \begin{cases} 2 & \text{if } i = j \text{ and } 2 \leq i \leq N-1 \\ 1 & \text{if } i = j \text{ for } i = 1, N \\ -1 & \text{if } |i-j| = 1. \end{cases}$$

The resulting closed-loop system is then

$$\ddot{x} = -r_1 L_{\text{ahead-path}}\dot{x} - r_0 L_{\text{undir-path}} x + u_{\text{ref}}(t). \tag{12}$$

The step responses for $N = 10, 100$ can be seen in Fig. 3a and 3b.

This can be compared to the serial consensus utilizing bidirectional information. For instance, if the forward-looking graph Laplacian $L_{\text{ahead-path}}$ is used together with the corresponding backward-looking graph Laplacian

$$(L_{\text{behind-path}})_{ij} = \begin{cases} 1 & \text{if } i = j \text{ and } i \leq N-1 \\ -1 & \text{if } i = j-1 \end{cases}.$$

The resulting closed-loop system is then

$$\ddot{x}(t) = -(p_1 L_{\text{ahead-path}} + p_2 L_{\text{behind-path}})\dot{x}(t) - p_1 p_2 L_{\text{ahead-path}} L_{\text{behind-path}} x(t) + u_{\text{ref}}(t). \tag{13}$$

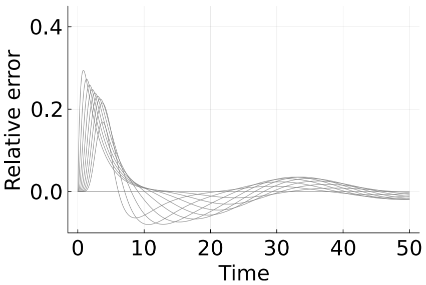

(a) Conventional consensus with symmetric position, asymmetric velocity feedback and $N = 10$.

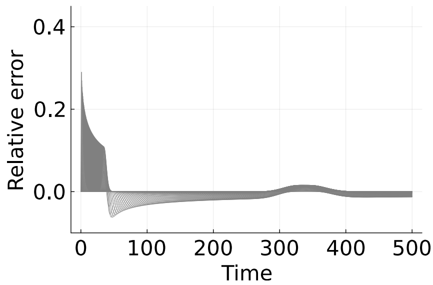

(b) Conventional consensus with symmetric position, asymmetric velocity feedback and $N = 100$.

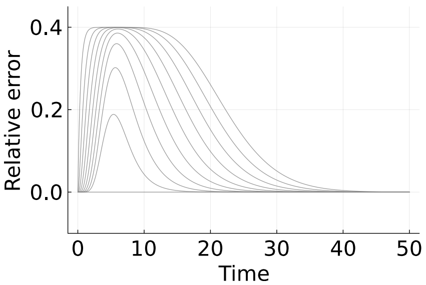

(c) Serial consensus with bidirectional feedback and $N = 10$.

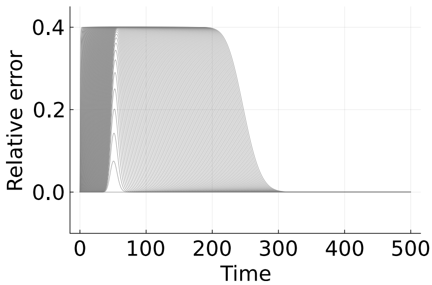

(d) Serial consensus with bidirectional feedback and $N = 100$.

Figure 3. Simulation of the initial value response to $x = 0$, $\dot{x}_{i\neq 1}(0) = 0$, and $\dot{x}_1(0) = 1$. The conventional consensus system (12) is considered with $r_1 = 2.5$ and $r_0 = 1$, while for the serial consensus system (13), $p_1 = 2$ and $p_2 = 0.5$ is used. The results illustrate that for some choices of graph Laplacians the serial and conventional consensus can have comparable performance.

The step responses can be seen in Fig. 3. From the figure we can observe that the serial consensus and conventional consensus can have similar transient performance. We find it is, however, easier to predict that the serial consensus will perform well, than various versions of the conventional protocol. Indeed, the protocol proposed by [Herman et al., 2017] is very similar to the serial consensus controller in Example 4.

6. Conclusions and directions for future work

In this paper we have introduced the serial consensus controller which is a distributed formation controller that achieves scalable stability, performance, and robustness. Here, scalability refers to the fact that these properties are independent of the formation size. The performance result is particularly important since it linearly bounds the $\|\cdot\|_\infty$-gain from the initial local errors and reference velocity deviation to the transient local errors and reference velocity deviations, measured in the same norm. This quantity, rather than, for example an L_2 gain, is directly related to the control and performance objectives. It is also worth noting that all of these results are achieved with only local relative measurements and linear feedback. The results are particularly interesting for large vehicle platoons where short inter-vehicle distances are desired and the transient behavior of the platoon is of great importance, though there are strict topological constraints (typically, those of a directed string). But, by virtue of the generality of the presented results they could also be of interest for other networked systems, such as power grids, sensor networks or multi-robot networks.

There are several interesting directions for future work. First, since the serial consensus may require an additional step of communication, an interesting question is whether this can be avoided, for instance through the use of local estimators. A second direction is to further investigate the robustness of the serial consensus, for instance with respect to time delays. Finally, implementation of serial consensus on a physical system is an interesting next step.

Appendix B

Here we will prove Theorem 11 and Proposition 12. The results are restated for convenience.

Proof of Theorem 11

Proof. i) Any square matrix can be unitarily transformed to upper triangular form by the Schur traingularization theorem. Let $U_k L_k U_k^H = T_k$ be upper triangular. Then the block diagonal matrix $U = \mathrm{diag}(U_1, U_2, \dots U_n)$ is a unitary matrix that upper triangularizes A in (8). For any triangular matrix the eigenvalues lie on the diagonal and this will be the eigenvalues of each $-L_k$. The result follows.

ii) First, consider the closed-loop dynamics of (6)

$$X(s) = (sI + L_1)^{-1}(sI + L_2)^{-1}U_{\text{ref}}(s).$$

Since, U_{ref} is stable, we know that the limit $\lim_{s\to 0} U_{\text{ref}}(s) = U_{\text{ref}}(0)$ exists. To prove that the system achieves second order consensus we want to show that

$$\lim_{t\to\infty} y(t) = \lim_{s\to 0} C(s)X(s) = 0$$

for some transfer matrix $C(s)$, which encodes the consensus states. But since the reference dependence is only related to $U_{\text{ref}}(0)$, we can simplify the problem to only consider impulse responses, which has the same transfer function as the initial value response where $\xi_n(0) = U_{\text{ref}}(0)$. Therefore, WLOG, assume that $U_{\text{ref}}(s) = 0$ and an arbitrary initial condition $\xi(0) = [\xi_1(0)^T, \xi_2^T(0)]^T$. The solution of (8) is given by $\exp(At)\xi(0) = S\exp(J(A)t)S^{-1}\xi(0)$ where $J(A)$ is the Jordan normal form of A and S is an invertible matrix. From i) and the diagonal dominance of the graph Laplacians we know that all eigenvalues of A lie in the left half plane. By Assumption A2 it follows that the zero eigenvalue for each L_k is simple. Now we prove that these two zero eigenvalues correspond to a Jordan block of size 2. Let $\mathbf{e}_1 = \begin{bmatrix}\mathbf{1}^T & 0\end{bmatrix}^T$ and $\mathbf{e}_2 = \begin{bmatrix}0 & \mathbf{1}^T\end{bmatrix}^T$. Then e_1 is an eigenvector since $A\mathbf{e}_1 = 0$. Now, since $e_1 = Ae_2$ combined with e_1 and e_2 being linearly independent it follows that they form a Jordan block of size 2 with an invariant subspace spanned by the vectors e_1 and e_2. All other eigenvectors make up an asymptotically stable invariant subspace, it follows that $\xi(t)$ will converge towards a solution in $\mathrm{span}(e_1, e_2)$ and thus $\lim_{t\to\infty}\xi_k(t) = \alpha_k(t)\mathbf{1}_N$. From $x(t) = \xi_1(t)$ we get $\lim_{t\to\infty} x(t) = \alpha_1(t)\mathbf{1}_N$, and furthermore, since

$$\dot{x} = \dot{\xi}_1 = -L_1\xi_1 + \xi_2 \to \xi_2 \text{ as } t \to \infty,$$

it follows that $\lim_{t\to\infty}\dot{x}(t) = \alpha_2(t)1_N$ which shows that the system achieves second order consensus. □

Proof of Proposition 2.

Proof. To prove this we must show that both $A_0, A_1 \in \mathcal{A}^2(W, c')$ where $A_0 = -L_2L_1$ and $A_1 = -(L_2 + L_1)$. First, A_1 and A_2 are shown to represent relative feedback. Since $L_1, L_2 \in \mathcal{A}^1(W, c)$, it holds that $A_0\mathbf{1} = -L_2L_1\mathbf{1} = -L_2\mathbf{0} = 0$ and similarly $A_1\mathbf{1} = -(L_2 + L_1)\mathbf{1} = 0$.

Second, we show that the gain is bounded. For the positional feedback we have

$$\|A_0\|_\infty = \|-L_2L_1\|_\infty \le \|L_2\|_\infty\|L_1\|_\infty \le c^2,$$

which followed from the submultiplicativity of the induced norm. For the velocity feedback

$$\|A_1\|_\infty = \|-(L_2 + L_1)\|_\infty \le \|L_2\|_\infty + \|L_1\|_\infty \le 2c,$$

where the triangle inequality was utilized. Let $c' = \max\{2c, c^2\}$, then clearly it holds true that both $\|A_0\|_\infty, \|A_1\|_\infty \le c'$.

Finally, we consider the sparsity pattern. Since W is non-negative, it follows that W^2 is also non-negative. Next, since adding non-negative elements to a matrix cannot remove any positive elements we get the following implications

$$\left[I{+}W{+}W^2\right]_{i,j}{=}0 \Longrightarrow [I{+}W]_{i,j}{=}0 \Longrightarrow [-L_1{-}L_2]_{i,j}{=}0,$$

which follows from the definition of $L_1, L_2 \in \mathcal{A}^1(W, c)$.

To show that $A_0 = -L_2L_1$ will be sparse, we note that any graph Laplacian can be written as $L = D - W$, where D is a diagonal matrix and W is non-negative. Thus we will consider the sparsity of

$$-(D_2 - W_2)(D_1 - W_1) = -D_2D_1 + D_2W_1 + W_2D_1 - W_2W_1.$$

Since multiplication with a diagonal matrix preserves sparsity, it clearly holds true that the first three terms satisfy

$$[I+W]_{i,j}=0 \Longrightarrow [-D_2D_1+D_2W_1+W_2D_1]_{i,j}=0.$$

For W_2W_1 we can introduce a non-negative matrix E such that $[W_{1,2}+E]_{i,j}=0 \iff W_{i,j}=0$ and in particular this construction ensures that $[(W_1+E)(W_2+E)]_{i,j}=0 \iff [W^2]_{i,j}$. Consider the following expanded product

$$(W_2+E)(W_1+E)=W_2W_1+W_2E+EW_1+E^2,$$

where all terms are products of non-negative matrices and are therefore also non-negative. It thus holds that $[W^2]_{i,j} \implies [W_2W_1]_{i,j}=0$. Combining the results for A_0 shows that

$$\left[I+W+W^2\right]_{i,j}=0 \implies [L_2L_1]_{i,j}=0.$$

This concludes the proof. □

References

Bamieh, B., M. R. Jovanovic, P. Mitra, and S. Patterson (2012). "Coherence in large-scale networks: dimension-dependent limitations of local feedback". *IEEE Transactions on Automatic Control* **57**:9, pp. 2235–2249.

Barooah, P., P. G. Mehta, and J. P. Hespanha (2009). "Mistuning-based control design to improve closed-loop stability margin of vehicular platoons". *IEEE Transactions on Automatic Control* **54**:9, pp. 2100–2113.

Besselink, B. and S. Knorn (2018). "Scalable input-to-state stability for performance analysis of large-scale networks". *IEEE Control Systems Letters* **2**:3, pp. 507–512.

Darbha, S., S. Konduri, and P. R. Pagilla (2019). "Benefits of v2v communication for autonomous and connected vehicles". *IEEE Transactions on Intelligent Transportation Systems* **20**:5, pp. 1954–1963.

Fax, J. A. and R. M. Murray (2004). "Information flow and cooperative control of vehicle formations". *IEEE Trans. Autom. Control* **49**:9, pp. 1465–1476.

Feintuch, A. and B. Francis (2012). "Infinite chains of kinematic points". *Automatica* **48**:5, pp. 901–908.

Feng, S., Y. Zhang, S. E. Li, Z. Cao, H. X. Liu, and L. Li (2019). "String stability for vehicular platoon control: definitions and analysis methods". *Annual Reviews in Control* **47**, pp. 81–97.

Hansson, J. and E. Tegling (2023). "A closed-loop design for scalable high-order consensus". In: *2023 IEEE Conf. on Decision and Control*. Accepted.

Herman, I., S. Knorn, and A. Ahlén (2017). “Disturbance scaling in bidirectional vehicle platoons with different asymmetry in position and velocity coupling”. *Automatica* **82**, pp. 13–20.

Jadbabaie, A., J. Lin, and A. Morse (2003). “Coordination of groups of mobile autonomous agents using nearest neighbor rules”. *IEEE Transactions on Automatic Control* **48**:6, pp. 988–1001.

Oh, K.-K., M.-C. Park, and H.-S. Ahn (2015). “A survey of multi-agent formation control”. *Automatica* **53**, pp. 424–440. ISSN: 0005-1098. DOI: `https://doi.org/10.1016/j.automatica.2014.10.022`. URL: `https://www.sciencedirect.com/science/article/pii/S0005109814004038`.

Olfati-Saber, R. and R. M. Murray (2004). “Consensus problems in networks of agents with switching topology and time-delays”. *IEEE Trans. Autom. Control* **49**:9, pp. 1520–1533.

Pasqualetti, F., S. Zampieri, and F. Bullo (2014). “Controllability metrics, limitations and algorithms for complex networks”. In: *2014 American Control Conf.* Pp. 3287–3292. DOI: `10.1109/ACC.2014.6858621`.

Patterson, S. and B. Bamieh (2014). “Consensus and coherence in fractal networks”. *IEEE Transactions on Control of Network Systems* **1**:4, pp. 338–348.

Ren, W. and E. Atkins (2007). “Distributed multi-vehicle coordinated control via local information exchange”. *International Journal of Robust and Nonlinear Control* **17**:10-11, pp. 1002–1033. DOI: `https://doi.org/10.1002/rnc.1147`. eprint: `https://onlinelibrary.wiley.com/doi/pdf/10.1002/rnc.1147`. URL: `https://onlinelibrary.wiley.com/doi/abs/10.1002/rnc.1147`.

Seiler, P., A. Pant, and K. Hedrick (2004). “Disturbance propagation in vehicle strings”. *IEEE Transactions on Automatic Control* **49**:10, pp. 1835–1842.

Siami, M. and N. Motee (2016). “Fundamental limits and tradeoffs on disturbance propagation in large-scale dynamical networks”. *IEEE Trans. Autom. Control* **61**:12, pp. 4055–4062.

Stüdli, S., M. Seron, and R. Middleton (2017a). “From vehicular platoons to general networked systems: string stability and related concepts”. *Annual Reviews in Control* **44**, pp. 157–172.

Stüdli, S., M. M. Seron, and R. H. Middleton (2017b). “Vehicular platoons in cyclic interconnections with constant inter-vehicle spacing”. *IFAC-PapersOnLine* **50**:1. 20th IFAC World Congress, pp. 2511–2516.

Swaroop, D. and J. Hedrick (1996). “String stability of interconnected systems”. *IEEE Trans. Autom. Control* **41**:3, pp. 349–357.

Tegling, E., B. Bamieh, and H. Sandberg (2023). “Scale fragilities in localized consensus dynamics”. *Automatica* **153**, p. 111046.

Tegling, E., P. Mitra, H. Sandberg, and B. Bamieh (2019). “On fundamental limitations of dynamic feedback control in regular large-scale networks”. *IEEE Transactions on Automatic Control* **64**:12, pp. 4936–4951.

Zhou, K. and J. C. Doyle (1998). *Essentials of robust control*. Vol. 104. Prentice hall Upper Saddle River, NJ.

Paper III

Input-Output Pseudospectral Bounds for Transient Analysis of Networked and High-Order Systems

Jonas Hansson **Emma Tegling**

Abstract

Motivated by a need to characterize transient behaviors in large network systems in terms of relevant signal norms and worst-case input scenarios, we propose a novel approach based on existing theory for matrix pseudospectra. We extend pseudospectral theorems, pertaining to matrix exponentials, to an input-output setting, where matrix exponentials are pre- and post-multiplied by input and output matrices. Analyzing the resulting transfer functions in the complex plane allows us to state new upper and lower bounds on system transients. These are useful for higher-order matrix differential equations, and specifically control of double-integrator networks such as vehicle formation problems. Therefore, we illustrate the theory's applicability to the problem of vehicle platooning and the question of string stability, and show how unfavorable transient behaviors can be discerned and quantified directly from the input-output pseudospectra.

The authors are with the Department of Automatic Control and the ELLIIT Strategic Research Area at Lund University, Lund, Sweden.

This work was partially funded by Wallenberg AI, Autonomous Systems and Software Program (WASP) funded by the Knut and Alice Wallenberg Foundation and the Swedish Research Council through Grant 2019-00691.

1. Introduction

Characterizing dynamic properties of systems with structure, in particular, network structure, is a long-standing problem in the field. While questions of stability and convergence have dominated the literature since the early works [Fax and Murray, 2004; Olfati-Saber and Murray, 2004], important questions pertaining to the performance and robustness of network systems are increasingly gaining attention. For example, [Bamieh et al., 2012] and later [Siami and Motee, 2016; Tegling et al., 2019] have described fundamental limitations to the performance of large networks subject to structural (sparsity) constraints, stated in terms of system norms.

A particular area where dynamic behaviors have received more attention is that of vehicle platooning, that is, the control of strings of vehicles, see [Levine and Athans, 1966; Chu, 1974] for early works. Here, it is fundamentally important to prevent disturbance propagation through the string (to avoid collisions!), and therefore, to have uniform bounds on error amplifications during transients. This has motivated the notion of *string stability*, see e.g., [Swaroop and Hedrick, 1996; Seiler et al., 2004] or [Stüdli et al., 2017; Feng et al., 2019] for more recent surveys. Conditions for string stability fall, roughly speaking, into two categories: 1) bounding the amplification of a disturbance from vehicle i to vehicle j, or 2) requiring that bounded initial errors lead to bounded output errors, independently of the string length. The choice of signal norms, however, is central for the bounds in this literature, and the interpretations they allow for. Many works have done analyses based on $\mathcal{L}_2$ to $\mathcal{L}_2$ string stability, see [Herman et al., 2017; Seiler et al., 2004; Ploeg et al., 2014] while the, as argued e.g. in [Feintuch and Francis, 2012], possibly more important $\mathcal{L}_\infty$ to $\mathcal{L}_\infty$ disturbance amplification has received significantly less attention even if considered in [Swaroop and Hedrick, 1996; Chu, 1974]. In this work, we shed light on a new approach to analyzing such bounds for input-output systems in general, and networks and vehicle strings in particular.

This approach takes off from the literature on *pseudospectra*. Pseudospectra, which complement spectral analysis of linear systems, especially for those with non-normal operators, have seen usage in describing the transient behavior of both differential and difference equations. The works are too numerous to mention, but we refer to [Trefethen and Embree, 2005] for an excellent textbook on the subject. Through pseudospectra one can state lower and upper bounds on the transient of the exponential matrix, i.e., on $\sup_{t\geq 0}\|e^{t\mathcal{A}}\|$, and thereby on the solution to a linear differential equation. In other words, on the transient response of the internal states of a linear system. The most famous such bounds are given by the Kreiss theorem [Kreiss, 1962]. However, in control, and in particular, network applications including vehicle platooning, we are not necessarily interested in the transients of the internal states. For instance, vehicular formation dynamics tend to have a double integrator rendering certain internal states unbounded, while inter-vehicular distances may be well-behaved. To cope with this one can incorporate measurement and input matrices $\mathcal{C}, \mathcal{B}$ and then bound $\sup_{t\geq 0} \|\mathcal{C}e^{t\mathcal{A}}\mathcal{B}\|$ instead.

The extension of pseudospectral bounds to such an input-output setting is the main focus of the present work. For this purpose we will define a notion of *input-output pseudospectra*. These will, in the case of higher-order systems (by which we mean systems with more than one integrator), become closely related to *structured* pseudospectra, which have been studied in [Tisseur and Higham, 2001; Lancaster and Psarrakos, 2005] and applied to mechanical systems in [Green et al., 2006]. In these works the main focus has been on the robustness of solutions to matrix polynomial equations including the quadratic eigenvalue problem. The related analysis of transient behavior of $\|\mathcal{C}e^{tA}\mathcal{B}\|$ has, to the best of our knowledge, barely received attention, though some structured Kreiss-like theorems were proven in [Matsuo, 1994; Plischke, 2005].

This paper aims to highlight the potential usefulness of the pseudospectral framework for networked systems and systems with higher-order dynamics. Platooning, where vehicles are modeled as double integrators (the acceleration is actuated), and which have a string network topology, is a prototypical example. We first generalize certain key results from [Trefethen and Embree, 2005] to an input-output setting. Furthermore, we use complex analysis to derive new upper bounds on the transients of state space realizations, which are especially useful for systems that have high-order dynamics. The generalizations lead to lower and upper bounds on the transient $\sup_{t\geq 0} \|\mathcal{C}e^{t\mathcal{A}}\mathcal{B}\|$, which under given input scenarios imply bounds on the output $\sup_{t\geq 0} \|y(t)\|$ (in any p-norm). Through examples we show how the new bounds can be applied. For a large-scale platooning problem, we compute bounds on the deviations from equilibrium for a worst-case bounded initial condition.

The remainder of this paper is organized as follows. In Sec. 2 we introduce the preliminaries of this work. Lower and upper bounds on the transient of $\sup_t \|y(t)\|$ and simple examples illustrating how to apply the bounds are presented in Sec. 3. Then we illustrate an application of our results in the form of vehicle strings in Sec. 4. Lastly our conlusions are presented in Sec. 5.

2. Preliminaries

Consider the linear time-invariant system

$$\begin{aligned} \dot{\xi}(t) &= \mathcal{A}\xi(t) + \mathcal{B}u(t) \\ y(t) &= \mathcal{C}\xi(t), \end{aligned} \tag{1}$$

where the state $\xi \in \mathbb{R}^N$, $\mathcal{A} \in \mathbb{R}^{N\times N}$, $\mathcal{B} \in \mathbb{R}^{N\times P}$, $\mathcal{C} \in \mathbb{R}^{Q\times N}$, and output $y \in \mathbb{R}^Q$. The initial condition is $\xi(0) = \xi_0$. We will interpret $\mathcal{C}(sI - \mathcal{A})^{-1}\mathcal{B}$ as a transfer matrix and call the system (1) input-output stable if all poles of this transfer matrix lie in the open left half plane. Denote by $\sigma(\mathcal{A})$ the spectrum, i.e., the set of eigenvalues of $\mathcal{A}$.

We will often let the system in (1) model matrix differential equations of the form

$$\begin{aligned} x^{(l)}(t) + A_{l-1}x^{(l-1)}(t) + \cdots + A_0 x(t) &= Bu(t) \\ y(t) &= \mathcal{C}\xi(t), \end{aligned} \tag{2}$$

where $x(t) \in \mathbb{R}^n$ and $x^{(k)}$ denotes the k^{th} time derivative of x: $x^{(k)}(t) = \frac{\mathrm{d}^k x(t)}{\mathrm{d}t^k}$. In this case, $\xi(t) = [x, \dot{x}, \ldots, x^{(l-1)}]^\top \in \mathbb{R}^{nl}$, with $nl = N$. This system can be equivalently stated on block-companion form as

$$\begin{aligned} \dot{\xi}(t) &= \underbrace{\begin{bmatrix} 0 & I_n & 0 & \ldots \\ \vdots & \ddots & \ddots & 0 \\ 0 & \ldots & 0 & I_n \\ -A_0 & -A_1 & \ldots & -A_{l-1} \end{bmatrix}}_{\mathcal{A}} \xi(t) + \underbrace{\begin{bmatrix} 0 \\ \vdots \\ 0 \\ B \end{bmatrix}}_{\mathcal{B}} u(t) \\ y(t) &= \mathcal{C}\xi(t). \end{aligned} \tag{3}$$

2.1 Signal and system norms

Norms are central to this work. Here we will consider the standard vector p-norms:

$$\|x\|_p = \begin{cases} \left(\sum_{k=1}^N |x_k|^p\right)^{\frac{1}{p}} & \text{if } 1 \le p < \infty \\ \max_k |x_k| & \text{if } p = \infty, \end{cases}$$

where $x \in \mathbb{C}^N$. For matrices we consider the corresponding induced norms, i.e.

$$\|\mathcal{A}\| = \sup_{\|x\|=1} \|\mathcal{A}x\|,$$

where $\mathcal{A} \in \mathbb{C}^{M\times N}$.

In general, our results can be interpreted in any of these norms and we will often omit the subscript to indicate that the results are valid for all of them. What we need for our theorems is, more specifically, that the matrix norms are submultiplicative, which means that the following inequality is valid for any two compatible matrices $A_1,\ A_2$

$$\|A_1 A_2\| \le \|A_1\|\|A_2\|.$$

It is well known that this is true for all the p-norms.

2.2 Input-output scenarios

We will present bounds in terms of the scaled exponential matrix $\mathcal{C}e^{\mathcal{A}t}\mathcal{B}$. Its norm can be seen as bounds on the transient response of the system (1) in the following scenarios:

Impulse response Consider the input signal $\{u(t) = \delta(t)u_0\}$ with $u_0 \in \mathbb{R}^P$ and let $||u_0|| = 1$ in some norm. The solution of (1) is given by

$$y(t) = \mathcal{C}e^{t\mathcal{A}}\mathcal{B}u_0 \tag{4}$$

and the worst possible transient of $y(t)$ is given by

$$\sup_t \|y(t)\| = \sup_t \sup_{\|u_0\|=1} \|\mathcal{C}e^{t\mathcal{A}}\mathcal{B}u_0\| = \sup_t \|\mathcal{C}e^{t\mathcal{A}}\mathcal{B}\|.$$

Response to an initial condition An initial condition response is given by

$$y(t) = \mathcal{C}e^{t\mathcal{A}}\xi(0).$$

To study the worst possible initial condition with respect to resulting deviations in the output $y(t)$ we may consider

$$\sup_t \|y(t)\| = \sup_t \sup_{\|\xi_0\|=1} \|\mathcal{C}e^{t\mathcal{A}}\xi_0\| = \sup_t \|\mathcal{C}e^{t\mathcal{A}}\|.$$

The corresponding analysis for the worst-case *structured* initial condition is done by multiplying ξ_0 by $\mathcal{B}$. In this case,

$$\sup_t \|y(t)\| = \sup_t \sup_{\|\xi_0\|=1} \|\mathcal{C}e^{t\mathcal{A}}\mathcal{B}\xi_0\| = \sup_t \|\mathcal{C}e^{t\mathcal{A}}\mathcal{B}\|.$$

For example, $\mathcal{B} = (I, 0, \ldots, 0)^T$ in (3) corresponds to all initial derivatives being zero.

2.3 Complex analysis

The basis for our upcoming theorems is three Laplace transform results, which were also used to derive key results in [Trefethen and Embree, 2005]. For completeness they are also presented.

Lemma 14 ([Trefethen and Embree, 2005, Theorem 15.1]) Let $\mathcal{A}$ be a matrix. There exist $\omega \in \mathbb{R}$ and $M \geq 1$ such that

$$\|e^{t\mathcal{A}}\| \leq Me^{\omega t} \qquad \forall t \geq 0. \tag{5}$$

Any $s \in \mathbb{C}$ with $Re s > \omega$ is in the resolvent set of $\mathcal{A}$, with

$$(sI - \mathcal{A})^{-1} = \int_0^\infty e^{-st}e^{t\mathcal{A}}\mathrm{d}t. \tag{6}$$

If $\mathcal{A}$ is a matrix or bounded operator, then

$$e^{t\mathcal{A}} = \frac{1}{2\pi i}\int_\Gamma e^{st}(sI-\mathcal{A})^{-1}\mathrm{d}s, \tag{7}$$

where Γ is any closed and positively oriented contour that encloses $\sigma(\mathcal{A})$ once in its interior.

2.4 Pseudospectra

Pseudospectra have proven themselves to be a useful tool for analysing the transient behavior and robustness of differential equations, see e.g. [Green et al., 2006]. There are several equivalent definitions of the pseudospectra of a matrix $\mathcal{A} \in \mathbb{C}^{N\times N}$. Two equivalent and well known are:

Definition 9 (ϵ-pseudospectra)

$$\sigma_\epsilon(\mathcal{A}) = \{s \in \mathbb{C} \mid \|(sI-\mathcal{A})^{-1}\| > \epsilon^{-1}\} \tag{8}$$

and

Definition 10 (ϵ-pseudospectra)

$$\sigma_\epsilon(\mathcal{A}) = \{s \in \mathbb{C} \mid s \in \sigma(\mathcal{A}+E)\dots \\ \dots \textit{for some } E \in \mathbb{C}^{N\times N} \textit{ with } \|E\| < \epsilon\}, \tag{9}$$

where $\sigma(\mathcal{A})$ denotes the (usual) spectrum of a matrix $\mathcal{A}$. We will also make use of the ϵ-pseudospectral abscissa, defined as $\alpha_\epsilon = \sup_{s\in\sigma_\epsilon} \mathrm{Re}\, s$.

From the two definitions of σ_ϵ we can get an idea of what they are used for. The first relates to the size of the resolvent and enables complex analysis in line with Lemma 14. The latter relates to the robustness of the matrix under perturbations. By considering level curves of pseudospectra for various ϵ-levels it is possible to get an understanding of the solutions of the linear differential equation $\dot{x}(t) = \mathcal{A}x(t)$ and of how sensitive the system is to perturbations.

When one is concerned with the transient behaviour of an input-output system as defined in (1) it will be proven useful to generalize Definition 9 in the following way:

Definition 11 (Input-output ϵ-pseudospectra)

$$\sigma_\epsilon(\mathcal{A},\mathcal{B},\mathcal{C}) = \{s \in \mathbb{C} \mid \|\mathcal{C}(sI-\mathcal{A})^{-1}\mathcal{B}\| > \epsilon^{-1}\}. \tag{10}$$

The corresponding input-output *pseudospectral abscissa* we define as

$$\alpha_\epsilon(\mathcal{A},\mathcal{B},\mathcal{C}) = \sup_{s\in\sigma_\epsilon(\mathcal{A},\mathcal{B},\mathcal{C})} \mathrm{Re}(s).$$

We also define the input-output spectrum $\sigma(\mathcal{A},\mathcal{B},\mathcal{C})$ as the set of poles of the transfer matrix $\mathcal{C}(sI-\mathcal{A})^{-1}\mathcal{B}$.

2.5 Kreiss theorem

The transient behavior of a matrix exponential for a stable matrix $\mathcal{A} \in \mathbb{R}^{N\times N}$ can be bounded through the so called *Kreiss bounds* [Trefethen and Embree, 2005, Thrm. 18.5]:

$$\mathcal{K}(\mathcal{A}) \leq \sup_{t\geq 0} \|e^{t\mathcal{A}}\| \leq eN\mathcal{K}(\mathcal{A}). \tag{11}$$

Here the Kreiss constant is defined as

$$\mathcal{K}(\mathcal{A}) = \sup_{\text{Re}s>0} \text{Re}s\|(sI-\mathcal{A})^{-1}\|. \tag{12}$$

Comparing (12) to Definition 1, the relation between the Kreiss bound and pseudospectra becomes evident. In fact, it holds that $\mathcal{K}(\mathcal{A}) = \sup_{\epsilon>0} \alpha_\epsilon/\epsilon$. In a controls context, it is natural to not only consider the matrix exponential, but rather an input-output setting. We therefore define the input-output Kreiss constant

$$\mathcal{K}(\mathcal{A},\mathcal{B},\mathcal{C}) = \sup_{\text{Re}s>0} \text{Re}s\|\mathcal{C}(sI-\mathcal{A})^{-1}\mathcal{B}\| = \sup_{\epsilon>0} \frac{\alpha_\epsilon(\mathcal{A},\mathcal{B},\mathcal{C})}{\epsilon}. \tag{13}$$

3. Input-Output Transient Bounds

We now make use of the theory in the previous section to derive bounds on the transient performance of the system (1), under the input-output scenarios introduced earlier. We will give both lower and upper bounds. As a starting point, consider the following proposition, which is a simple but important extension to Lemma 14:

Proposition 15 Let $\mathcal{A}$, $\mathcal{B}$ and $\mathcal{C}$ be matrices and let $\|\cdot\|$ denote a submultiplicative norm. There exist $w \in \mathbb{R}$ and $M \geq \|\mathcal{C}\mathcal{B}\|$ such that

$$\|\mathcal{C}e^{t\mathcal{A}}\mathcal{B}\| \leq Me^{\omega t} \qquad \forall t \geq 0. \tag{14}$$

Any $s \in \mathbb{C}$ with $Res > \omega$ is in the resolvent set of $\mathcal{A}$, with

$$\mathcal{C}(sI-\mathcal{A})^{-1}\mathcal{B} = \int_0^\infty e^{-st}\mathcal{C}e^{t\mathcal{A}}\mathcal{B}\text{d}t, \tag{15}$$

$$\mathcal{C}e^{t\mathcal{A}}\mathcal{B} = \frac{1}{2\pi i}\int_\Gamma e^{st}\mathcal{C}(sI-\mathcal{A})^{-1}\mathcal{B}\text{d}s, \tag{16}$$

and where Γ is any closed and positively oriented contour that encloses $\sigma(\mathcal{A},\mathcal{B},\mathcal{C})$ once in its interior.

Proof. First, (14) follows from the norm's submultiplicativity and (5) as

$$\|\mathcal{C}e^{t\mathcal{A}}\mathcal{B}\| \leq \|\mathcal{C}\|\|\mathcal{B}\|\|e^{t\mathcal{A}}\| \leq \|\mathcal{C}\|\|\mathcal{B}\|\hat{M}e^{wt},$$

with $M = \|\mathcal{C}\|\|\mathcal{B}\|\hat{M}$. Letting $t = 0$ yields $\|\mathcal{C}\mathcal{B}\| \leq M$.

Next, (15) follows from linearity of the integral, i.e., the fact that for any compatible matrices B, C, and $f(x)$ we have $B\int(f(x)\mathrm{d}x)C = \int Bf(x)C\mathrm{d}x$.

Last, consider (16). Through linearity and (7), we get

$$\mathcal{C}e^{t\mathcal{A}}\mathcal{B} = \frac{1}{2\pi i}\int_{\Gamma'} e^{st}\mathcal{C}(sI-\mathcal{A})^{-1}\mathcal{B}\mathrm{d}s,$$

where Γ' encircles $\sigma(A)$. If $\sigma(\mathcal{A},\mathcal{B},\mathcal{C}) = \sigma(\mathcal{A})$ we are done. If not, suppose that there are n_p distinct poles $s_p \in \sigma(A)$ such that $s_p \notin \sigma(\mathcal{A},\mathcal{B},\mathcal{C})$. Let Γ' be the union of Γ and n_p disjoint circles with radius ϵ with the poles s_p at the center. Let ϵ be sufficiently small such that the ϵ-circles are disjoint from $\sigma(\mathcal{A},\mathcal{B},\mathcal{C})$. Now, since the transfer matrix $\mathcal{C}(sI-\mathcal{A})^{-1}\mathcal{B}$ does not contain any poles in the interior of the ϵ-discs, each of the transfer functions is holomorphic in each disc enclosed by the ϵ-circles. By the maximum modulus principle they cannot have any strict local maximum in the interior of each ϵ-disc. This implies that there is an $M_\epsilon \geq 0$ such that each transfer function $|(\mathcal{C}(sI-\mathcal{A})^{-1}\mathcal{B})_{i,j}| \leq M_\epsilon$. In turn, this implies that $\|e^{st}(\mathcal{C}(sI-\mathcal{A})^{-1}\mathcal{B})\|_\infty \leq e^{Re(s_p+\epsilon)t}M_\epsilon P$ on any circle γ, where P is the number of columns of $\mathcal{B}$. The curve integral is thus bounded by $\int_\gamma \|\mathcal{C}(sI-\mathcal{A})^{-1}\mathcal{B}\|_\infty \mathrm{d}s \leq Pe^{Re(s_p+\epsilon)t}M_\epsilon \epsilon 2\pi$, which then converges to 0 as $\epsilon \longrightarrow 0$. This is true for all n_p circles and so we can ignore the part encircling the non-observable poles. By equivalence of norms, this is true for any p-norm. □

We will now make use of Proposition 15 to state upper and lower bounds on the quantity $\sup_{t\geq 0}\|\mathcal{C}e^{t\mathcal{A}}\mathcal{B}\|$.

3.1 Lower bound

We begin by stating a lower bound analogous to the lower bound in the Kreiss theorem (11). Despite its relevance to control systems, this extension of the Kreiss theorem has, to our knowledge, not been observed in the literature apart from [Matsuo, 1994] and [Plischke, 2005]. The short proof we present here, however, is new.

Theorem 16—Lower bound

$$\sup_{t\geq 0}\|\mathcal{C}e^{t\mathcal{A}}\mathcal{B}\| \geq \sup_{Res>0} Res\|\mathcal{C}(sI-\mathcal{A})^{-1}\mathcal{B}\| \tag{17}$$

Proof. Let $M = \sup_{t\geq 0}\|\mathcal{C}e^{t\mathcal{A}}\mathcal{B}\|$ and $\mathrm{Re}s > 0$. From (15) we have

$$\|\mathcal{C}(sI-\mathcal{A})^{-1}\mathcal{B}\| = \|\int_0^\infty e^{-st}\mathcal{C}e^{t\mathcal{A}}\mathcal{B}\mathrm{d}t\|$$

$$\implies \|\mathcal{C}(sI-\mathcal{A})^{-1}\mathcal{B}\| \leq M\int_0^\infty e^{-t\mathrm{Re}s}\mathrm{d}t = \frac{M}{\mathrm{Re}s},$$

multiplying both sides by $\mathrm{Re}s$ proves the inequality. □

The theorem reveals that the input-output Kreiss constant $\mathcal{K}(\mathcal{A},\mathcal{B},\mathcal{C})$ defined in (13) can lower bound the transient of the system (1) under the input scenarios in Sec. 2.2.

3.2 Upper bounds

Now we present three ways to bound the transient from above, again, using Proposition 15 as a basis for the proofs.

THEOREM 17—FIRST UPPER BOUND
If $\mathcal{A}$, $\mathcal{B}$, $\mathcal{C}$ are matrices and L_ϵ is the arc length of the boundary of $\sigma_\epsilon(\mathcal{A},\mathcal{B},\mathcal{C})$ or of its convex hull for some $\epsilon > 0$, then

$$\|\mathcal{C}e^{t\mathcal{A}}\mathcal{B}\| \leq \frac{L_\epsilon e^{t\alpha_\epsilon(\mathcal{A},\mathcal{B},\mathcal{C})}}{2\pi\epsilon}, \tag{18}$$

where $\alpha_\epsilon(\mathcal{A},\mathcal{B},\mathcal{C}) = \sup\{Re s \mid \|\mathcal{C}(s-\mathcal{A})^{-1}\mathcal{B}\| > \epsilon^{-1}\}$.

Proof. For any closed contour Γ enclosing $\sigma_\epsilon(\mathcal{A},\mathcal{B},\mathcal{C})$ we have (16). Taking the norm on both sides gives

$$\begin{aligned}\|\mathcal{C}e^{t\mathcal{A}}\mathcal{B}\| &= \left\|\frac{1}{2\pi i}\int_\Gamma e^{st}\mathcal{C}(sI-\mathcal{A})^{-1}\mathcal{B}\mathrm{d}s\right\| \\ &\leq \frac{1}{2\pi}\int_\Gamma \|e^{st}\mathcal{C}(sI-\mathcal{A})^{-1}\mathcal{B}\|\mathrm{d}s \leq \frac{L_\epsilon e^{t\alpha_\epsilon(\mathcal{A},\mathcal{B},\mathcal{C})}}{2\pi\epsilon}.\end{aligned}$$

The second inequality follows since $\|\mathcal{C}(sI-\mathcal{A})^{-1}\mathcal{B}\| \leq \epsilon^{-1}$ along Γ. The convex hull can be used to reduce the length L_ϵ of Γ. This is possible as $\|\mathcal{C}(sI-\mathcal{A})^{-1}\mathcal{B}\| \leq \epsilon^{-1}$ on the boundary of the convex hull. □

Theorem 17 is a fairly straightforward extension of [Trefethen and Embree, 2005, Theorem 15.2]. However, we next present a novel alternative characterization which will prove useful, in particular for classes of higher-order matrix differential equations.

THEOREM 18—SECOND UPPER BOUND
Let the system (1) with $(\mathcal{A},\mathcal{B},\mathcal{C})$ be input-output stable and let $R = a\|\mathcal{A}\|$ for some $a > 1$. Then

$$\|\mathcal{C}e^{t\mathcal{A}}\mathcal{B}\| \leq \frac{1}{2\pi}\int_{-R}^{R}\|\mathcal{C}(i\omega-\mathcal{A})^{-1}\mathcal{B}\|d\omega + \frac{\|\mathcal{C}\|\|\mathcal{B}\|}{2-2a^{-1}} \tag{19}$$

Proof. By definition of input-output stability all poles of the transfer matrix $\mathcal{C}(sI-\mathcal{A})^{-1}\mathcal{B}$ lie in the left half plane. Furthermore, the spectrum $\sigma(\mathcal{A})$ is contained in the disc $|s| \leq \|\mathcal{A}\|$ since for any eigenvector x of $\mathcal{A}$ with $\|x\| = 1$ we have $\|\mathcal{A}\| \geq \|\mathcal{A}x\| = |\lambda|$. Now take Γ to be the semicircle with radius $R > \|A\|$ that goes up the imaginary axis and then extends into the left half plane. Then this Γ encloses the input-output spectrum $\sigma(\mathcal{A},\mathcal{B},\mathcal{C})$ and (16) yields

$$\begin{aligned}\|\mathcal{C}e^{t\mathcal{A}}\mathcal{B}\| &\leq \frac{1}{2\pi}\int_\Gamma e^{t\mathrm{Re}(s)}\|\mathcal{C}(s-\mathcal{A})^{-1}\mathcal{B}\|\mathrm{d}s \\ &\leq \frac{1}{2\pi}\int_{-R}^{R}\|\mathcal{C}(i\omega-\mathcal{A})^{-1}\mathcal{B}\|\mathrm{d}\omega \\ &+\frac{1}{2\pi}\int_{\pi/2}^{3\pi/2}\|\mathcal{C}(Re^{i\theta}-\mathcal{A})^{-1}\mathcal{B}\|R\mathrm{d}\theta.\end{aligned}$$

If $|s| = \|\mathcal{A}\|a$ and $a > 1$, then, the integral in the second term can be bounded using the following series expansion of the inverse:

$$\|(sI-\mathcal{A})^{-1}\| = \left\|\frac{1}{s}\sum_{k=0}^{\infty}\left(\frac{\mathcal{A}}{s}\right)^k\right\| \leq \frac{1}{\|\mathcal{A}\|}\frac{1}{a-1}$$

This, together with submultiplicativity yield $\|\mathcal{C}(Re^{i\theta}-\mathcal{A})^{-1}\mathcal{B}\|R \leq \|\mathcal{C}\|\mathcal{B}\|\|\mathcal{A}\|a\frac{1}{\|\mathcal{A}\|}\frac{1}{a-1}$ which can be used to upper bound the second integral to $\frac{\|\mathcal{C}\|\|\mathcal{B}\|}{2-2a^{-1}}$. □

Now we will look into another bound, similar in its nature.

Theorem 19—Third Upper bound
Let the system (1) with $(\mathcal{A},\mathcal{B},\mathcal{C})$ be input-output stable. If $\|\mathcal{C}(sI-\mathcal{A})^{-1}\mathcal{B}\| \leq M|s|^{-\beta}$ for all $|s| \geq K$ for some $\beta > 1$, $M > 0$, and $K > 0$. Then

$$\|\mathcal{C}e^{t\mathcal{A}}\mathcal{B}\| \leq \frac{1}{2\pi}\int_{-\infty}^{\infty}\|\mathcal{C}(i\omega-\mathcal{A})^{-1}\mathcal{B}\|\mathrm{d}\omega < \infty. \tag{20}$$

Proof. Taking the norm of (16), we get

$$\|\mathcal{C}e^{t\mathcal{A}}\mathcal{B}\| \leq \frac{1}{2\pi}\int_\Gamma \|e^{st}\mathcal{C}(sI-\mathcal{A})^{-1}\mathcal{B}\|\mathrm{d}s.$$

Now, use the same semicircle Γ as in the proof of Theorem 18 with radius $R > \|\mathcal{A}\|$. This Γ encloses the input-output spectra $\sigma(\mathcal{A},\mathcal{B},\mathcal{C})$. Furthermore if $R > K$ we have

$$\begin{aligned}\|\mathcal{C}e^{t\mathcal{A}}\mathcal{B}\| &\leq \frac{1}{2\pi}\lim_{R\to\infty}\left(\int_{-R}^{R}\|e^{i\omega t}\mathcal{C}(i\omega-\mathcal{A})^{-1}\mathcal{B}\|d\omega+\pi RMR^{-\beta}\right) \\ &= \frac{1}{2\pi}\int_{-\infty}^{\infty}\|\mathcal{C}(i\omega-\mathcal{A})^{-1}\mathcal{B}\|d\omega,\end{aligned}$$

where the last equality follows from the condition $\beta > 1$. □

The condition on β in Theorem 19 can be related to the relative degree of the system. For instance, if $\mathcal{C}(sI-\mathcal{A})^{-1}\mathcal{B}=(s^2I+sA_1+A_0)^{-1}$ and is input-output stable, then $\beta=2$ and it is possible to apply the theorem.

The usefulness of the three upper bounds boils down to the fact that the spectrum is usually difficult to characterize. For the first bound (18), a good description of the pseudospectra is needed, while in the second and third bounds (19)–(20) good knowledge of the resolvent along the imaginary axis is needed. We will clarify through two simple examples.

Example 7 Consider the dynamical system

$$\begin{aligned}\dot{\xi}&=\begin{bmatrix}0 & 1\\ -1 & -2\end{bmatrix}\xi+\begin{bmatrix}0\\1\end{bmatrix}u\\ y&=\begin{bmatrix}1 & 0\end{bmatrix}\xi.\end{aligned} \tag{21}$$

Suppose we are interested in the impulse response of the system. Then we have

$$\mathcal{C}(sI-\mathcal{A})^{-1}\mathcal{B}=\frac{1}{(s+1)^2}.$$

In this case we can see that the ϵ-level curves of $\|\mathcal{C}(sI-\mathcal{A})^{-1}\mathcal{B}\|=1/\epsilon$ are given by the circles $|s+1|=\sqrt{\epsilon}$. From (18) we see that the upper bound for each ϵ is

$$\|\mathcal{C}e^{tA}\mathcal{B}\|\le\frac{2\pi\sqrt{\epsilon}e^{t(-1+\sqrt{\epsilon})}}{2\pi\epsilon}=\frac{e^{t(-1+\sqrt{\epsilon})}}{\sqrt{\epsilon}}.$$

The lowest upper bound is achieved for $\epsilon=1$ and is simply $\|Ce^{t\mathcal{A}}\mathcal{B}\|\le 1$.

The third upper bound (Theorem 19) requires input-output stability, which is clearly satisfied. The relative degree is 2 which implies $\beta=2>1$. To calculate the bound (20) we need to calculate the integral along the imaginary axis. In this case

$$\begin{aligned}\|\mathcal{C}e^{t\mathcal{A}}\mathcal{B}\|&\le\frac{1}{2\pi}\int_{-\infty}^{\infty}\|\mathcal{C}(\omega iI-\mathcal{A})^{-1}\mathcal{B}\|\mathrm{d}\omega\\ &=\frac{1}{\pi}\int_0^{\infty}\frac{1}{\omega^2+1}\mathrm{d}\omega=\frac{1}{2}\end{aligned}$$

A lower bound of this system can be calculated by only considering the real axis (and in this case this is also optimal). This leads to optimizing

$$\sup_{t\ge0}\|\mathcal{C}e^{t\mathcal{A}}\mathcal{B}\|\ge\sup_{x>0}\left\|\frac{x}{(x+1)^2}\right\|=\frac{1}{4}.$$

Since this system is very simple it is also possible to calculate the actual maximum which is $\sup_{t\ge0}\|\mathcal{C}e^{t\mathcal{A}}\mathcal{B}\|=1/e$.

As demonstrated above, Theorem 19 is useful if the relative degree of the system transfer function is greater than 1. Now we show a case where where we cannot use this theorem.

EXAMPLE 8 *Consider the same system (21) as before, but now the response to a non-zero initial value* $\xi(0) = [x_0, 0]^\top$. *This can be represented by* $\mathcal{B} = [1,0]^T$. *Then we have*

$$\mathcal{C}(sI - \mathcal{A})^{-1}\mathcal{B} = \frac{s+2}{(s+1)^2}.$$

To calculate our first upper bound in (18) we need to encircle the spectrum. The shape here is non-trivial but at least we know that for any circle centered around -1 *with radius smaller than* 1 *we have*

$$\left|\frac{s+2}{(s+1)^2}\right| \le \left|\frac{2}{(s+1)^2}\right|.$$

The previous calculations give us the upper bound $\|\mathcal{C}e^{t\mathcal{A}}\mathcal{B}\| \le 2$. *In this case we cannot use Theorem 19 since the relative degree is* 1 *and therefore* $\beta \le 1$. *However, we can use the very similar Theorem 18 to give an upper bound.* $\|\mathcal{A}\|_\infty = 3$ *and so for any* $R > 3$ *we can use the theorem. It remains to calculate the curve integral along the imaginary axis. Doing this with numerical integration for* $R = 9$ *yields the upper bound* $\|\mathcal{C}e^{tA}\mathcal{B}\| \lessapprox 2.025$ *(Through optimization this bound can be lowered to* $\|\mathcal{C}e^{tA}\mathcal{B}\| \lessapprox 2.023$*)*

Through these examples we have shown that the best upper bound depends on the situation. The upside of using Theorems 18 and 19 is that they are quite easy to compute numerically. Theorems 16 and 17 relate to the level curves of the input-output pseudospectra and can be qualitatively seen through inspection of these curves, as we will demonstrate in the next section.

4. Application to networks: vehicle strings

To illustrate our bounds, we consider the problem of controlling a string of vehicles – the platooning problem. While performance bounds on platoons and their relation to the network or interaction structure has received ample attention, as we stated in the introduction, the problem calls for bounds relating to the quantity $\sup_t \|y(t)\|_\infty$, where y captures a displacement error. Bounds of this type are important, especially in platooning, since they directly relate to the allowable spacing between consecutive vehicles. However, they tend to be difficult to derive analytically. Here we illustrate how our pseudospectra-inspired approach can be used to evaluate string stability properties for various platoon structures in terms of this quantity.

For this purpose, consider a platoon of size n where each unit is modelled as a double integrator in one spatial dimension, i.e.

$$\ddot{x}_k = u_k$$

where x_k is the position of the kth vehicle with respect to a fix reference and u_k is the input force at vehicle k.

To control the platoon we consider a control law that depends on relative distances to neighboring vehicles and relative to a speed reference. For $k \in \{2,\dots,n-1\}$ we get:

$$u_k = (1+\beta_d)(\dot{x}_{k-1}-\dot{x}_k)-(1-\beta_d)(\dot{x}_k-\dot{x}_{k+1})+\alpha(v_{\text{ref}}-\dot{x}_k) \\ +(1+\beta_p)(x_{k-1}-x_k-d)-(1-\beta_p)(x_k-x_{k+1}-d), \quad (22)$$

where β_d and β_p are parameters capturing the degree of symmetry in the control law (i.e., look-ahead vs. look-behind control), d a desired intervehicle spacing, v_{ref} is a velocity reference, and $\alpha \geq 0$ is a weight. For the first and last vehicles, we simply define $\ddot{x}_1 = -(1-\beta_d)(\dot{x}_1-\dot{x}_2)+\alpha(v_{\text{ref}}-\dot{x}_1)-(1-\beta_p)(x_1-x_2-d)$, $\ddot{x}_n = (1+\beta_d)(\dot{x}_{n-1}-\dot{x}_n)+\alpha(v_{\text{ref}}-\dot{x}_n)+(1+\beta_p)(x_{n-1}-x_n-d)$. By considering the translated dynamics $\hat{x}_k = x_k + kd$ we get the same dynamics as if we assume $d=0$, so for simplicity we set $d=0$ and consider the dynamics around this equilibrium.

The closed-loop system can be written:

$$\begin{bmatrix}\dot{x}\\ \ddot{x}\end{bmatrix} = \begin{bmatrix}0 & I\\ -L_p & -L_d-\alpha I\end{bmatrix}\begin{bmatrix}x\\ \dot{x}\end{bmatrix}+\begin{bmatrix}0\\ \alpha\mathbf{1}\end{bmatrix}v_{\text{ref}} = \mathcal{A}\xi+\mathcal{B}v_{\text{ref}}.$$
$$y = \begin{bmatrix}C & 0\end{bmatrix}\begin{bmatrix}x\\ \dot{x}\end{bmatrix} = \mathcal{C}\xi, \quad (23)$$

where $L_p,\ L_d \in \mathbb{R}^{n\times n}$ are graph Laplacians capturing the vehicle interactions (see further down for definitions). This and similar systems are well studied, see e.g. [Stüdli et al., 2017].

A way to ensure the platoon is well-behaved (e.g. string stable) is to make α large in comparison to L_d and L_p. This, however, essentially transforms the problem to an open-loop system, which is obviously problematic in a real-world setting with disturbances and measurement noise or bias. This motivates the use of a fairly small α, allowing the inter-vehicle adjustments to dominate. In this example, we will use $\alpha = 0.1$.

We use the framework from Section 3 to analyze this system for two cases, one where both Laplacians are asymmetric (a directed string) and one where both are symmetric (bidirectional string). For each system we consider the output

$$y = \begin{bmatrix}x_1-x_2\\ x_{\lfloor N/2\rfloor}-x_{\lfloor N/2\rfloor+1}\\ x_{n-1}-x_n\end{bmatrix},$$

which samples three inter-vehicle distances: at the start, middle, and end of the platoon. We will consider the initial condition response, i.e. $\mathcal{B} = I_{2n}$. We expect a string unstable system to perform poorly for at least one of these outputs.

One merit of our proposed method is the possibility to analyze very large systems. In both cases considered here, we therefore model a platoon of $n = 400$ vehicles. We remark that it would of course be possible to simulate the systems for many different inputs and through simulation bound the possible outputs. But as n grows, this quickly becomes very computationally heavy. Using our theorems generates bounds on the worst case input without any additional effort.

4.1 Directed vehicle string

Consider the control law (22) with $\beta_p = \beta_d = 1$, which renders it fully asymmetric. In this case, we obtain in (23) $L_p = L_d = L_{\text{asym}}$, with

$$L_{\text{asym}} = \begin{bmatrix} 0 & & & \\ -2 & 2 & & \\ & \ddots & \ddots & \\ & & -2 & 2 \end{bmatrix}. \tag{24}$$

In Fig. 1 we show the shape of the input-output pseudospectra corresponding to an initial condition response, that is, the level curves of the quantity $\|\mathcal{C}(sI-\mathcal{A})^{-1}I_{2n}\|_\infty$ of (23) with $n = 400$ vehicles. We can see that the level curves extend far into the right half plane with magnitudes of order 10^{30} where $\text{Re}(s)$ is of order 10^{-1}. Through the lower bound in Theorem 16 we can immediately see that there will be a large transient of $\|y(t)\|_\infty$ in at least the orders of 10^{29}. Through a line search, starting at the maximum along the imaginary axis and going into the right half plane we learn that the lower bound in amplification from the worst-case initial conditions to the output (see Section 2.2) is at least

$$\sup_{t\geq 0} \|y(t)\|_\infty \gtrapprox 4.3 \cdot 10^{31},$$

for some ξ_0 such that $\|\xi_0\|_\infty \leq 1$.

Fig. 2 displays a Bode plot of the system for various platoon sizes n. That is, we plot the amplitude $\|\mathcal{C}(sI-\mathcal{A})^{-1}I_{2n}\|_\infty$ for $s = i\omega$, $\omega \in (0,\infty)$. Here, we can see the extreme amplification of the frequency response close to the frequency $\omega = 1$. According to our Theorem 18, we can use this frequency response to calculate an upper bound on the transient through integration. By numerical integration we can estimate the upper bound to be

$$\sup_{t\geq 0} |y(t)\|_\infty \lessapprox 1.4 \cdot 10^{33}.$$

From these two bounds we can already conclude that this topology is not suitable for a string of vehicles.

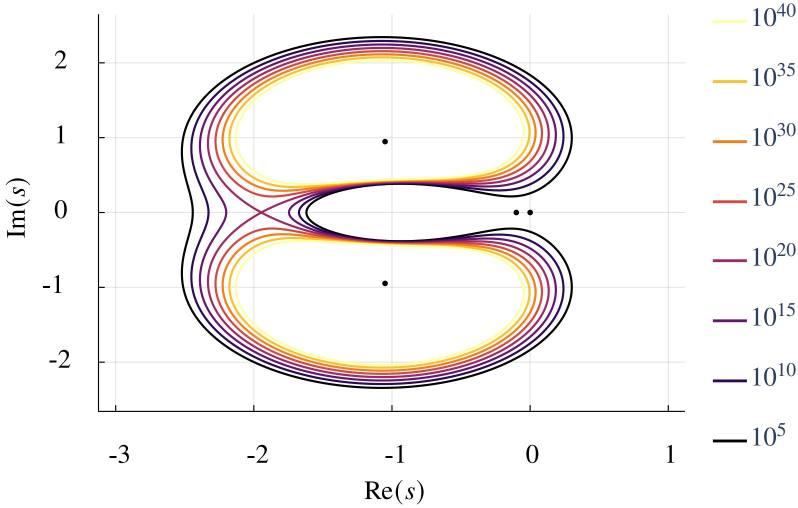

Figure 1. The input-output pseudospectra of (23) for a directed vehicle string with $n = 400$ vehicles. The black dots are the eigenvalues of $\mathcal{A}$. The large values of the input-output pseudospectra even for small s in the right half plane indicate an unfavorable lower bound in Theorem 16.

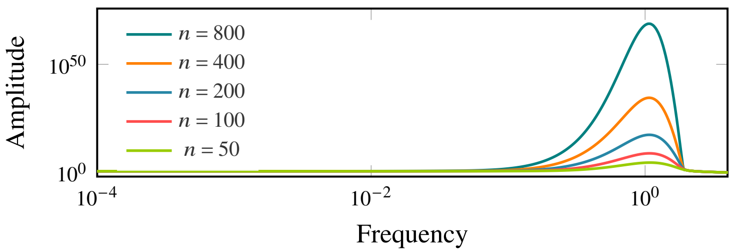

Figure 2. Bode plot displaying the worst-case frequency response of (23) for a directed vehicle string. The amplitude is measured in $\|\cdot\|_\infty$ and the response is shown for various platoon lengths n.

Remark 5 The bounds were possible to compute, since the inversion $\mathcal{C}(sI - \mathcal{A})^{-1}$ can be reduced to the sparse problem $C(s^2 I + sL_d + L_p)^{-1}$, where $C \in \mathbb{R}^{3,n}$. As L_d and L_p are tridiagonal this can be computed in $\mathcal{O}(n)$ operations.

4.2 Bidirectional (symmetric) vehicle string

Now, let $\beta_d = \beta_p = 0$ in (22), leading to the symmetric Laplacians $L_p = L_d = L_{\text{sym}}$, with

$$L_{\text{sym}} = \begin{bmatrix} 1 & -1 & & & \\ -1 & 2 & -1 & & \\ & \ddots & \ddots & \ddots & \\ & & -1 & 2 & -1 \\ & & & -1 & 1 \end{bmatrix}. \tag{25}$$

This corresponds to a bidirectional string of vehicles. In Fig. 3 we show the shape of the input-output pseudospectra corresponding to an initial condition response of (23) with $n = 400$ vehicles. We can see that the input-output spectra is quite well-behaved and do not extend far into the right half plane, indicating transients will be modest. By Theorem 16 and a line search along the real axis, we learn that the lower bound in amplification from initial conditions to output is

$$\sup_{t \geq 0} \|y(t)\|_\infty \gtrapprox 2.2,$$

for some ξ_0 such that $\|\xi_0\|_\infty \leq 1$.

In Fig. 4 we can see the frequency response calculated for various n. Interestingly, the common slope among the curves seems to only behave like a square root which would mean that there is an upper bound independent of the platoon length which bounds the transients due to arbitrary non-zero initial conditions. The numerical upper bound when $n = 400$ was calculated to

$$\sup_{t \geq 0} |\mathcal{C}e^{t\mathcal{A}}\xi_0\|_\infty \lessapprox 9.3.$$

This can be compared with the upper bound calculated for $n = 10^6$ which evaluated at 9.4.

5. Conclusions

In this work we have proposed a pseudospectra-based approach to analyze transient performance of input-output systems, and generalized existing bounds for this purpose. Through our bounds it is possible to quantify $\sup_{t \geq 0} \|\mathcal{C}e^{t\mathcal{A}}\mathcal{B}\|$ in terms of lower and upper bounds. These can be seen as bounding the performance from a worst-case input disturbance to an output $y(t)$ in any p-norm – otherwise often intractable to study. Regarding the problem of controlling vehicle strings in Sec. 4, we illustrated one application where we believe our bounds can be useful, opening the door to future analysis. For instance, deriving analytical bounds for special network structures. The theorems can also be used to numerically calculate bounds for network structures where the worst inputs are non-obvious, for instance when the agents are non-homogeneous or interaction matrices non-normal.

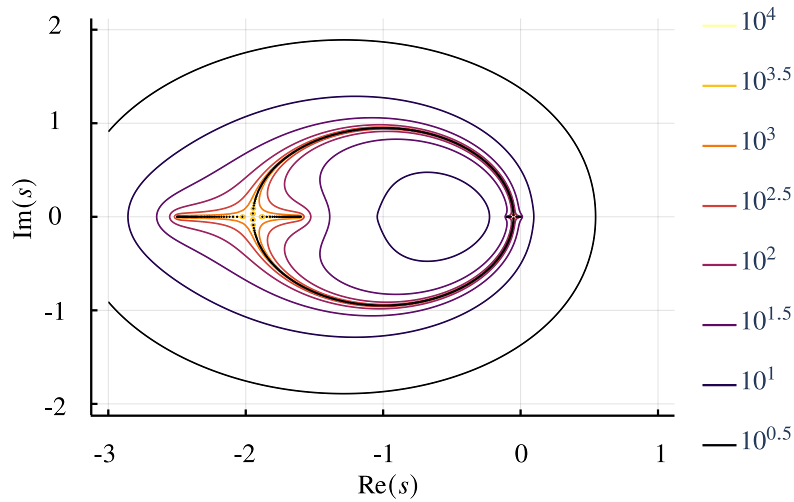

Figure 3. The input-output pseudospectra of (23) for a bidirectional vehicle string with $n = 400$ vehicles. The black dots are the eigenvalues of $\mathcal{A}$. The level curve corresponding to $\|\mathcal{C}(sI - \mathcal{A})^{-1}\| = 10^{1.5}$ can be roughly inscribed in a 1 radius circle, which hints through Theorem 17 that the transients of $\|y(t)\|_\infty$ will be small.

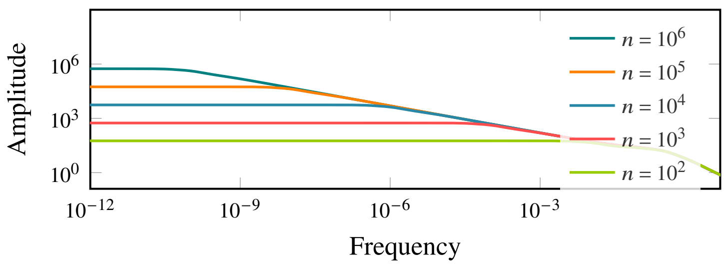

Figure 4. Bode plot displaying the worst-case frequency response of (23) for a bidirectional vehicle string. The amplitude is measured in $\|\cdot\|_\infty$ and the response is shown for various platoon lengths n.

References

Bamieh, B., M. R. Jovanovic, P. Mitra, and S. Patterson (2012). "Coherence in large-scale networks: dimension-dependent limitations of local feedback". *IEEE Trans. Autom. Control* **57**:9, pp. 2235–2249.

Chu, K.-c. (1974). "Decentralized control of high-speed vehicular strings". *Transportation Science* **8**:4, pp. 361–384.

Fax, J. A. and R. M. Murray (2004). "Information flow and cooperative control of vehicle formations". *IEEE Trans. Autom. Control* **49**:9, pp. 1465–1476.

Feintuch, A. and B. Francis (2012). "Infinite chains of kinematic points". *Automatica* **48**:5, pp. 901–908.

Feng, S., Y. Zhang, S. E. Li, Z. Cao, H. X. Liu, and L. Li (2019). "String stability for vehicular platoon control: definitions and analysis methods". *Annual Reviews in Control* **47**, pp. 81–97.

Green, K., A. Champneys, and M. Friswell (2006). "Analysis of the transient response of an automatic dynamic balancer for eccentric rotors". *Int. J. Mech. Sci.* **48**:3, pp. 274–293. ISSN: 0020-7403.

Herman, I., S. Knorn, and A. Ahlén (2017). "Disturbance scaling in bidirectional vehicle platoons with different asymmetry in position and velocity coupling". *Automatica* **82**, pp. 13–20.

Kreiss, H.-O. (1962). "Über die stabilitätsdefinition für differenzengleichungen die partielle differentialgleichungen approximieren". *BIT Numerical Mathematics* **2**, pp. 153–181.

Lancaster, P. and P. Psarrakos (2005). "On the pseudospectra of matrix polynomials". *SIAM J. Matrix Anal. Appl.* **27**:1, pp. 115–129.

Levine, W. and M. Athans (1966). "On the optimal error regulation of a string of moving vehicles". *IEEE Trans. Autom. Control* **11**:3, pp. 355–361.

Matsuo, T. (1994). "Some transfer-function conditions for a desired maximum amplitude or exponential envelope of a closed-loop transient response". In: *IEEE Conf. on Decision and Control*. Vol. 3, pp. 2659–2660.

Olfati-Saber, R. and R. M. Murray (2004). "Consensus problems in networks of agents with switching topology and time-delays". *IEEE Trans. Autom. Control* **49**:9, pp. 1520–1533.

Plischke, E. (2005). *Transient Effects of Linear Dynamical Systems*. PhD thesis. University of Bremen.

Ploeg, J., N. van de Wouw, and H. Nijmeijer (2014). "Lp string stability of cascaded systems: application to vehicle platooning". *IEEE Trans. Control Syst. Technol.* **22**:2, pp. 786–793.

Seiler, P., A. Pant, and K. Hedrick (2004). "Disturbance propagation in vehicle strings". *IEEE Transactions on Automatic Control* **49**:10, pp. 1835–1842.

Siami, M. and N. Motee (2016). “Fundamental limits and tradeoffs on disturbance propagation in large-scale dynamical networks”. *IEEE Trans. Autom. Control* **61**:12, pp. 4055–4062.

Stüdli, S., M. Seron, and R. Middleton (2017). “From vehicular platoons to general networked systems: string stability and related concepts”. *Annual Reviews in Control* **44**, pp. 157–172.

Swaroop, D. and J. Hedrick (1996). “String stability of interconnected systems”. *IEEE Trans. Autom. Control* **41**:3, pp. 349–357.

Tegling, E., P. Mitra, H. Sandberg, and B. Bamieh (2019). “On fundamental limitations of dynamic feedback control in regular large-scale networks”. *IEEE Trans. Autom. Control* **64**:12, pp. 4936–4951.

Tisseur, F. and N. J. Higham (2001). “Structured pseudospectra for polynomial eigenvalue problems, with applications”. *SIAM J. Matrix Anal. Appl.* **23**:1, pp. 187–208.

Trefethen, L. N. and M. Embree (2005). *Spectra and Pseudospectra: The Behavior of Nonnormal Matrices and Operators*. Princeton University Press, Princeton.